A DIGITAL APPROACH TO SHIP-HELICOPTER OPERATIONS CLEARANCE

Christopher Dadswell, Nicholas Fernandez, Mark D White, Neale Watson, Daniel Newton-Young, David Souza Branco, Daniella York, Dylan Coyle, Ieuan Owen,
University of Liverpool, Liverpool, United Kingdom
John Goodby, Leonardo Helicopters, Yeovil, United Kingdom

Abstract

Clearance of helicopters to naval vessels is a complex, costly and at times hazardous process which could be significantly improved by application of Modelling and Simulation (M&S). Building on established capabilities for ship-air integration modelling, the authors present a new framework for generating digital evidence to support the UK Ministry of Defence (MoD) ship air-release process. The framework applies independent fidelity assessment of both air and ship system models to build credibility of integrated simulations that may lack applicable validation data. The framework is developed to ensure outputs comply with RA 5812, the MoD and Military Aviation Authority's regulatory article governing use of M&S in airworthiness decision-making. To support compliance, specific fidelity metrics are proposed for key M&S based on existing literature and new experimental results that examine how variations in ship airwake characteristics affect helicopter deck landing performance. The framework is demonstrated using an initial case study involving the AW159 Wildcat and Type 23 frigate, which illustrates the approach and highlights fidelity sensitivities. Future work will refine and validate the M&S components to improve confidence in digital evidence for operational clearance decisions, and support qualification of future aircraft/ship pairings.

NOTATION

Symbols:

n_x, n_y, n_z	Aircraft load factor components, g
R_m	Main rotor radius, m
R_t	Tail rotor radius, m
s	Laplace operator
SF_{TI}	Turbulence intensity scale factor
SF_{vel}	Velocity scale factor
t	Time, s
TI	Turbulence Intensity
U_∞	Reference wind velocity, m/s
u, v, w	Airwake velocity components, m/s
w_n	White noise input
δ_{Lat}	Lateral control input, %
δ_{Long}	Longitudinal control input, %
δ_{Coll}	Collective control input, %
δ_{Ped}	Pedal control input, %
$\sigma_u, \sigma_v, \sigma_w$	Airwake velocity standard deviations
Ω, Ω_{TR}	Main, tail rotor speed of rotation, rad/s

Acronyms:

ACP	Airload Computation Point
ACR	Applicable Certification Rules
ADV	Acoustic Doppler Velocimeter
AS	Air System
BWR	Bedford Workload Rating
CAUM	Corrected All Up Mass
CFD	Computational Fluid Dynamics
CS	Certification Specification
DDES	Delayed-Detached Eddy Simulation
DIPES	Deck-Interface-Pilot-Effort-Scale
e-CETI	enhanced-Control Equivalent Turbulence Input
EASA	European Union Aviation Safety Agency
ERF	European Rotorcraft Forum
FSTD(H)	Flight Simulation Training Device (Helicopters)
FS	Flight Simulator
FSM	Flight Simulation Model
FS&T	Flight Science and Technology
FoCFT	First of Class Flight Trial
FoTFT	First of Type Flight Trial
FTMS	Flight Test Measurement System
HQ	Handling Qualities
HQR	Handling Qualities Rating

LH	Leonardo Helicopters
MAA	Military Aviation Authority
MECC	Minimum Expected Constituent Component
MoD	Ministry of Defence
M&S	Modelling and Simulation
MTE	Mission Task Elements
MUAD	Maximum Unnoticeable Added Dynamics
RTS	Release to Service
RA	Regulatory Article
RCAT	Rotorcraft Concepts & Tactical Aviation Research
RoCS	Rotorcraft Certification by Simulation
RWS	Real World System
SAI	Ship-Air Integration
SAIF	Ship Air Interface Framework
SA-R	Ship Air-Release
SA-RLE	Ship Air-Release with Limited Evidence
SFR	Simulator Fidelity Rating
SHOL	Ship Helicopter Operating Limits
SS	Ship System
SSM	Ship System Model
TP	Test Pilot
TFF	Transient Following a Failure
UoL	University of Liverpool
VAD	Virtual Air Dyn
V&V	Verification and Validation
WOD	Wind-Over-Deck

1 INTRODUCTION

Helicopters have become an essential tactical system for navies across the world, performing missions including resupply, reconnaissance, troop transport, search and rescue, and anti-submarine or surface warfare. However, launch and recovery of helicopters to ships at sea is both difficult and dangerous. The pitching, rolling and heaving motion of the flight deck, combined with unsteady airflow in the lee of the ship superstructure (referred to as the ship airwake), forms a challenging environment for pilots to navigate. Figure 1 illustrates the portside variant of the UK Royal Navy's standard forward-facing approach used for recovery of helicopters to ships.

The manoeuvre can be broadly split into four phases: a deceleration to hover alongside, a translation across deck, station keeping above the flight deck, and landing during an appropriate quiescent period in ship motion. These mission tasks are performed under a range of wind-over-deck (WOD) speeds and directions, with turbulence caused by the ship superstructure. Furthermore, these tasks expose a range of critical aircraft performance characteristics and handling qualities, including control trim and engine torque limits, attitude quickness, control power, control bandwidth and cross-couplings. As such, clearance of an Air System (AS) to a Ship System (SS) is a tightly regulated process to guarantee that the operational interface between two extremely complex and distinct systems is safe for front-line personnel.

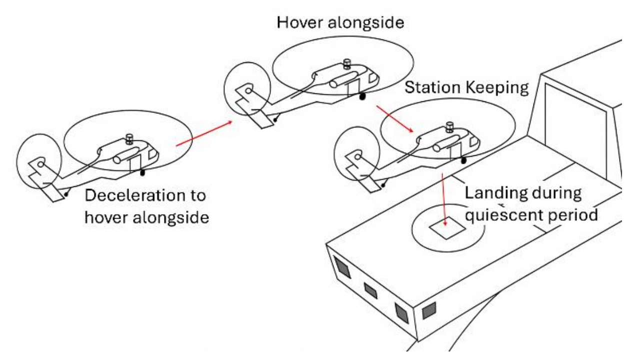

Figure 1: UK Royal Navy standard port-side forward-facing recovery approach to a single spot frigate.

1.1 Ship-Air Integration and Clearance

In the UK, the Ship-Air Integration (SAI) process is ultimately governed by the Ministry of Defence (MoD)'s Regulatory Article (RA) 1395 [1], which dictates the activities that must be completed by various stakeholders to generate two key permissions: the aircraft's Release to Service (RTS), and the Ship Air-Release (SA-R). The RTS is airworthiness clearance that provides the aircraft operator with aircraft applicable limitations, warnings and cautions for SAI, while the SA-R provides the ship operator with equivalent ship applicable information. Following the issuance of the SA-R, it is integrated into the Royal Navy's manual for embarked aviation operations, BRd 766 [2], and routine AS/SS operations can commence. Compliance must be demonstrated for a large range of requirements that are mostly related to the design of the two systems; most are straightforward to demonstrate by traditional means and will not be discussed in this paper. However, some requirements related to conduct of operations necessitate more involved testing, like establishment of the Ship-Helicopter Operating Limits (SHOL). Figure 2 shows a typical SHOL diagram for deployed operations, which limits launch and recoveries using the port-side forward-facing approach to a set of defined wind conditions, ship deck attitudes, helicopter Corrected All-Up-Mass (CAUM), and visibility conditions.

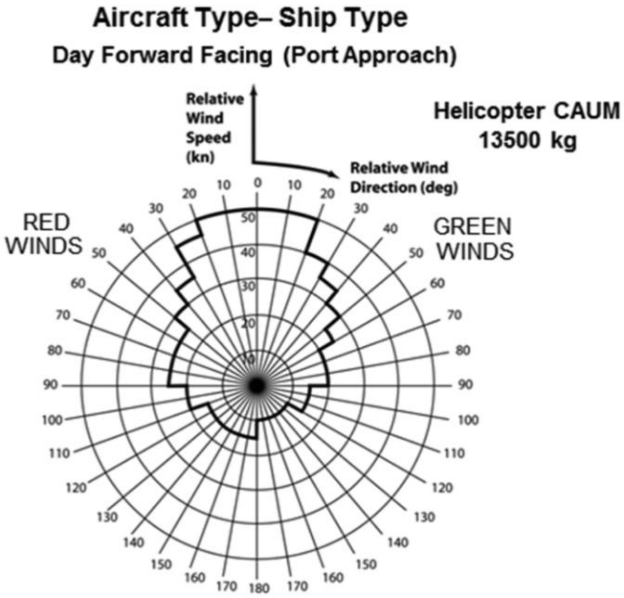

Max Pitch	Max Roll
±2°	±6°

Figure 2: Example SHOL showing wind over deck envelope for a UK port-side forward-facing landing manoeuvre [3]

As per Defence Standard 00-133, Aviation Arrangement in Surface Ships Part 4 [4], the SHOL for a given ship-aircraft combination is determined during a ship's First of Class Flight Trials (FoCFT) or an aircraft's First of Type Flight Trials (FoTFT). During these trials, Test Pilots (TP) perform and rate numerous launch and recovery tasks for winds of varying magnitude and direction. The TP ratings and recorded aircraft performance data are then used to demonstrate compliance with the applicable regulations, which are defined in Def. Stan. 00-970 Part 7: Certification Specifications for Airworthiness: Rotorcraft [5]. The operative section for SAI is Section 2.3.3.1, which is subdivided in three parts, containing:

a. A statement that the pilot must rate launch or recovery tasks with the Deck Interface Pilot Effort Scale (DIPES) described in Ref. [6]
b. A range of qualitative requirements on landing gear characteristics, rotorcraft agility, wind gust and turbulence response, Automatic Flight Control System configuration, and aircraft securing system characteristics;
c. Requirements that for a landing to be considered acceptable:
    1. The steady state and transient torque limits should not be exceeded
    2. The steady state and transient yaw control margins should not be less than 10% and 5% of total control range, respectively.

Further requirements on deck operations and rotor down-load are listed in paragraphs 2.3.3.2 and 2.3.3.3 of Ref. [5] that give maximum limits of wind and ship deck motion amongst other restrictions. Additionally, requirement UK29.479a defines minimum loads that the undercarriage must withstand in different sea states based on probability curves.

Many of these requirements, particularly those in 2.3.3.1, are traditionally only demonstrated during at-sea helicopter/ship flight testing. However, embarked trials are expensive, time consuming and hazardous, as pilots must attempt launch and recovery with limited prior knowledge of the potential hazards presented by the test conditions. The availability of conditions also often becomes a determining factor of the ultimate SHOL; a condition may be safe for launch/recovery, but if that condition cannot be tested during FoCFT then it will not be cleared in the SA-R. Therefore, limited availability of test conditions can lead to artificially restricted SHOL boundaries that can impact operational efficiency and effectiveness, solely due to inability to find particular winds during embarked trials.

1.2 Modelling & Simulation in Airworthiness Decision Making

The use of Modelling and Simulation (M&S) to supplement or replace embarked testing ahead of SA-R is attractive from cost and risk reduction perspectives, and can also expand operational capability. This approach is encouraged in Def. Stan. 00-133, which specifically recognises the utlity of Computational Fluid Dynamics (CFD) for accurately predicting air flow and air pattern over the ship deck. It also recommends systematic analysis of the AS as supporting evidence for FoCFT/FoTFT but the form of this analysis is not specified. The University of Liverpool (UoL) Flight Science and Technology (FS&T) research group has played a central role in advancing M&S of both helicopters and the ship-air interface, enabling the uses that Def. Stan. 00-133 advocates. FS&T's contributions include advancements to CFD-airwake generation [7], SAI analysis tools [8], [9] and piloted simulation processes [10]. Highlights in the application of these developments include studies on the Type 23 Frigate [11] and Type 45 Destroyer [12], the new UK Type 26 Frigate [13], and the Queen Elizabeth Class Aircraft Carrier [14]. However, these tools are still yet to be meaningfully applied in a real-world clearance process.

The MoD's RA 5812 [15] lays out a process to establish appropriate levels of development and assurance of M&S to enable its use in airworthiness decision-making. Hence, if any M&S evidence is to be used in support of RTS or SA-R development, both fundamentally airworthiness assessments, it must comply with RA 5812. The regulation borrows from NASA-STD-7009B [16], a technical standard that covers Verification & Validation (V&V) of M&S against a Real-World System (RWS), but aligns definitions with defence aviation. RA 5812 requires that the applicant consider the criticality of the M&S (a combination of the intended level of influence, and potential consequences), and demonstrate compliance with some selected standards or specification. The criticality is determined through a matrix construct given in Table 1, which defines a criticality level A through D, with A denoting high criticality to the M&S used.

Table 1: RA 5812 Criticality Matrix

Level of Influence					
	Controlling	B	B	A	A
	Significant	C	B	B	A
	Moderate	C	C	B	B
	Minor	D	C	C	B
	Negligible	D	D	C	C
		Minor	Major	Critical	Catastrophic
		Decision Consequence			

The criticality levels are aligned as follows:

A. The full set of requirements in the selected standard(s)/specification(s) must be applied and safety arguments developed to demonstrate the increased risks have been mitigated.
B. The full set of requirements in the selected standard(s)/specification(s) must be applied
C. Tailoring of the requirements from the selected standard(s) / specification(s) is permitted with agreement from the Military Airworthiness Authority (MAA).
D. Application of requirements from the selected standard(s) / specification(s) is discretionary and does not require MAA agreement.

Deciding which standards/specifications that should be applied to the M&S is left to the judgement of the user based on suitability to their application but does mandate that applied standards should cover ten Minimum Expected Constituent Components, given in Table 2. The authors view these ten components under two categories: technical and programmatic, i.e. elements that contain particular engineering challenges in compliance, and other elements that are important for M&S assurance but do not impart any technical challenges.

Table 2: RA 5812 minimum expected constituent components of a specification or standard

1.	Data and M&S input verification, validation and pedigree	**Technical**
2.	A mechanism for measuring compliance	
3.	Verification and validation for specific M&S	
4.	Uncertainty characterisation	
5.	Sensitivity analysis	
6.	Competence	**Programmatic**
7.	Processes for analysing and interpreting results	
8.	Change management processes	
9.	Processes for reporting results	
10.	Best practices for user interface design	

Selection of M&S standards that contain these expected components presents a unique challenge for SAI. As the name suggests, it is typically regarded as an interface of two disparate and complex models. While this approach is attractive to enable reuse of AS and SS models in different combinations, it complicates the definition of overarching standards for governing SAI fidelity. NASA-STD-7009B is an applicable standard, but as it only refers to general M&S, there are no compliance metrics or associated fidelity bounds that would be suitable for SAI models. Importantly, RA 5812 does allow for combinations of standards to be applied where a single relevant standard does not exist. Hence, standards that apply individually to the AS and SS models can be explored as options. Some standards for verification and validation of CFD models typically used for the SS do exist, such as the American society of Mechanical Engineers' (ASME) V&V 20-2009 [17], but the scope of ship airwake computation makes the standards difficult to apply. Standards such as the European Aviation Safety Authority (EASA)'s Certification Specific – Flight Simulation Training Device for Helicopters (CS-FSTD(H)) [18] provide fidelity standards for training simulators, but the basis for these requirements is often unclear and their sufficiency for M&S in certification or clearance applications is also unproven in isolation.

1.3 Rotorcraft Certification by Simulation

In the civilian arena, use of M&S in the certification of rotorcraft is emerging as a viable approach that can significantly reduce cost and risk in this often-lengthy process. The authors have significant experience in this field after playing a key role in the EU CleanSky2-funded Rotorcraft Certification by Simulation (RoCS) project. This project brought together researchers (UoL, Cranfield University, NLR, DLR, Politecnico di Milano), manufacturers (Leonardo Helicopters), and regulators (EASA) to develop a viable approach for digital certification.

Using Leonardo Helicopter's (LH) AW109 Trekker as an exemplar, RoCS developed a guidance manual [19] detailing an approach to certification by simulation and analysis characterised by three distinct phases:

Phase 1 – Requirements Capture and Specification

The process developed in RoCS begins with identification of the Applicable Certification Rules (ACRs) to be addressed through M&S, followed by two key decisions:

1. What level of certification credit is sought? I.e. full credit, partial credit, critical point analysis or de-risking evidence.
2. What conditions are to be assessed, and how do they relate to existing/anticipated validation data? I.e. will M&S be interpolating between known outcomes, or extrapolating beyond them?

These two questions are answered with a level between 1 and 4, which are combined in an 'influence-predictability' matrix to determine the overall level of confidence required in the M&S. This confidence level is then translated into specific requirements to be fed into phase 2 development.

Phase 2 – Flight Simulation Model (2A), Flight Simulator (2B) and Flight Test Measurement System (FTMS) Development

The second phase is sub-divided into three elements that deal with the mathematical Flight Simulation Model (FSM), physical Flight Simulator (FS), and Flight Test Measurement System (FTMS) used to capture data for validation of the FSM & FS. Parallel development of these distinct systems is required to enable important feedback loops between them, i.e. design of the FTMS must be informed by the validation requirements of the FSM, deficiencies in the FSM are often illuminated by piloted testing in the FS, and systems required in the FS may require specific development of the FSM. These feedback mechanisms allows for better coordination of testing procedures and outputs between the three elements, which is key for building a robust certification basis.

Phase 3 – Credibility Assessment

The final phase comprises actual performance of certification test points, and quantification of uncertainties in measurements taken. These two elements are brought together to build the certification case, i.e. this is the prediction of the system performance at the point of interest, and this is the confidence in that measurement. This evidence is then presented to the regulator for approval.

While RoCS successfully demonstrated application of the newly developed process against EASA certification specifications, it did not explore integration of ship models, or use military clearance processes, which typically present significantly different approaches to risk than civil equivalents. However, due to the common inspiration drawn from NASA-STD-7009B in development of both the RoCS guidance and the UK's RA 5812, there are significant overlaps in the evidence expected for both documents. Common factors like verification, validation and sensitivity and uncertainty analysis mean that mapping of the RoCS process to UK SA-R process is possible and useful, though application to other nations' ship-air clearance process may vary based on their regulatory frameworks.

To build on the RoCS developments and advance practical use of M&S in the SAI clearance process, FS&T are part of a consortium led by LH that was awarded a contract under Dstl's Rotorcraft Concepts & Tactical Aviation Research (RCAT) project. The aim of the project is to improve operational efficiency and capability through digital engineering, with a main problem statement for RCAT Work Package 2B "*to develop tools and metrics that enable consistent and convincing compliance with RA 5812*" in the context of ship air operations [20]. This paper will detail progress against that aim using an example ship and helicopter combination to demonstrate developed processes.

2 A DIGITAL FRAMEWORK FOR SHIP AIR-RELEASE

Under the RCAT2B project, the authors have proposed a new framework for development of digital SA-R evidence that allows for structured compliance with RA 5812. In partnership with LH, a staged application of the framework to several aircraft/ship combinations has also been planned, beginning with use of in-service systems to validate the process, before exploiting it against new platforms.

The clearance framework, shown in Figure 3, is structured to leverage a 70:20:10 approach; 70% of effort in any ship-helicopter qualification task is applied to 'offline' M&S analysis to validate component models and generate a predictive SHOL, 20% of effort is used on piloted simulation testing to generate a candidate SHOL, and 10% is used on at-sea testing for SAI M&S correlation, validation and verification purposes. This approach allows for significant cost savings and risk reduction against traditional at-sea ship-helicopter FoCFT/FoTFT qualification testing. The framework is characterised by independent development, verification and validation of the AS (further sub-divided to FSM and FS) and SS models before integrating the two. This ambitious approach builds layers of credibility into the final integrated simulation and boosts confidence in the eventual output. The process is inherently iterative, so that AS and SS models can be updated and improved in response to deficiencies found at the various assessment stages.

The integrated AS/SS models are evaluated both in an 'offline' mode, where desktop simulation tools are used to develop a predicted SHOL, and with 'online' tools for pilot-in-the-loop simulation to develop a candidate SHOL. Use of offline tools is intended to reduce scope of piloted testing through critical point analysis, and to provide more objective analysis of SAI M&S, rather than solely relying on subjective pilot opinion captured through ratings scales such as DIPES and the Simulator Fidelity Rating Scale (SFR) [21]. Once a candidate SHOL has been declared following combination of offline and piloted simulation outputs, it forms the foundation of a Ship Air-Release with Limited Evidence (SA-RLE), the regulatory clearance used to approve any embarked flight trial. Currently, it is assumed that embarked testing is still required to validate the M&S to some degree, but this can be significantly reduced in scope as test points are replaced with simulation evidence.

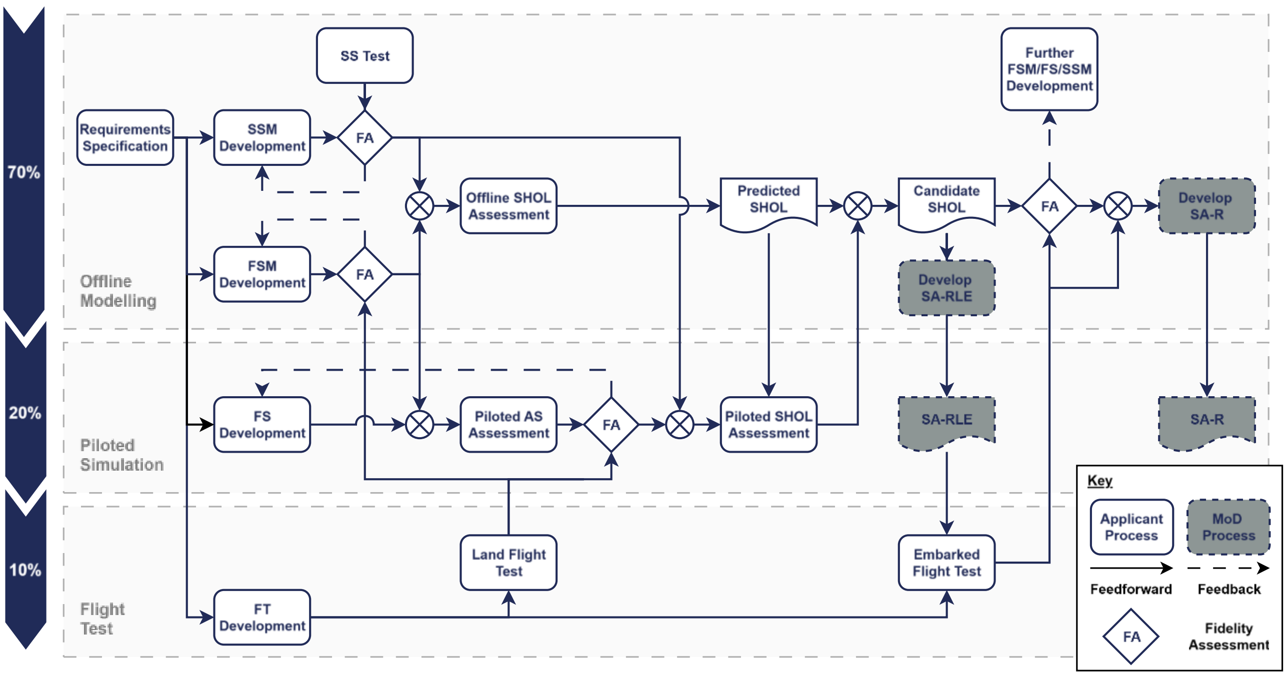

Figure 3: The proposed Ship Air Interface Clearance Framework developed during RCAT2B

At this juncture it is important to acknowledge that the framework may be applied in two primary modes:

1. Pre-FoCFT/FoTFT – no validation data is available, and candidate SHOL will inform all embarked testing.
2. Post-FoCFT/FoTFT envelope expansion/modification clearance – validation data has already been captured, so revised SA-R may be possible without further testing.

If operating in 'mode 1', some level of embarked testing must still be performed, and the fidelity of validation points in the candidate SHOL assessed before any of that evidence may be submitted for full SA-R. However, the scope of that testing may be drastically reduced to validate the M&S, rather than to fully define the SHOL. In future, even this may not be necessary if pedigree of previous work is sufficient for the regulator. The work described in this paper follows a validation exercise performed in 'mode 2', using existing validation data of the AW159 Wildcat and Type 23 frigate as exemplars, with no further embarked testing performed. As such, the flight test elements are not discussed in detail in this paper.

2.1 Criticality and Standards Selection

To inform standards selection and further requirements specification of M&S components, an intended M&S criticality level must be defined, as discussed in Section 1.2. Level of influence of a digitally-generated SHOL is intended to be significant at the least, and more likely controlling. Per the MAA definitions set out in RA 1210 [22], incorrect SHOL definition could lead to critical or catastrophic consequences due to the risk of pilot, crew or passenger fatalities. Hence, the anticipated criticality level is assessed as A, inferring that full standards/specifications must be applied with additional safety arguments. However, as previously discussed, there is no single applicable standard that can ensure adequate M&S fidelity in this case, so a combination must be applied, as permitted by RA 5812.

The authors propose a range of established quantitative and qualitative approaches to meet the Minimum Expected Constituent Component (MECCs) of RA 5812 and have commenced development of new standards where no appropriate ones could be found. The proposed standards and metrics are discussed for each of the framework components in the following sections with reference to each of the RA 5812 MECCs.

3 Flight Simulation Model & Flight Simulator

The FSM and FS are discussed together here due to their closely integrated nature, but per the framework are discrete entities. This is a key enabler for the 70:20:10 approach, where a majority of the analysis can be performed without pilot involvement.

3.1 Assessment Rationale and Methodology

The first RA 5812 MECC (data and input pedigree and V&V) requires traceability of all M&S input data to a valid source, with estimations of accuracy, precision and uncertainty for each parameter. These uncertainties form the foundation for later characterisation of uncertainty in model outputs and should also be used to inform sensitivity analysis. This process is similar regardless of particular use case, so the NASA-STD-7009B M&S data pedigree factor is proposed as a measure of compliance with this MECC across all components.

MECC 2, a mechanism for measuring compliance, is more difficult to define. The RoCS project provided exemplar methodologies for assessing model and simulator fidelity but also identified that an applicable unified standard does not exist. Efforts to apply a unified standard are also viewed as inappropriate given the wide range of requirements that might be addressed to different levels of influence and predictability. Hence, training requirements like CS-FSTD(H), while useful, have not been demonstrated to ensure sufficient fidelity for this clearance use in isolation. Therefore, an integrated approach to assessing FSM & FS fidelity using a range of predictive and perceived metrics is proposed using the RoCS approach.

While CS-FSTD(H) requirements are insufficient in isolation, they do provide some baseline of fidelity, so relevant sections to hover and low speed performance and handling qualities are applied here (detailed further below). To provide a more rigorous assessment of FSM fidelity, a quantitative handling qualities assessment was performed in the hover and low speed regime using ADS-33E-PRF Handling Qualities (HQ) metrics [23]. It is important to note that ADS-33E-PRF is primarily a handling qualities requirements document but is not applied here as requirements for the aircraft. Instead, the fidelity assessment approach described in Ref. [24] is applied, which correlated percentage difference in the ADS-33E-PRF quantitative metrics to variations in pilot performance of related Mission Task Elements (MTEs). It was further suggested that a nominal 10% tolerance on HQ metrics was appropriate for ensuring sufficient fidelity.

The authors also advocate using a Maximum Unnoticeable Added Dynamics (MUAD) approach based on error response functions in the frequency domain, as described in Ref. [25], and further developed in Ref. [26]. This approach has been demonstrated to provide limits on variation in aircraft frequency response before it creates a noticeable effect on pilot task performance, ideally suited for assessing potential impact of M&S fidelity deficiencies.

Applying the assessment methods above allows for predictive analysis of aircraft trim, stability and response (in both time and frequency domain), i.e. how well the model matches reality numerically. However, pilot perceived fidelity of the FS, and by extension the FSM, is also regarded as a critical measure of fidelity. RoCS advocated use of the Cooper Harper Handling Qualities Rating (HQR) scale as a validation metric, which is a subjective assessment tool to evaluate aircraft HQs based on pilot compensation and task performance against a standard using a 10-point scale [27]. ADS-33E-PRF defines a range of standard MTEs to be evaluated using Cooper-Harper which are commonly performed during military rotorcraft type certification. This enables comparative assessment of the MTEs in the FS where matching HQRs to the RWS infers equivalent levels of task performance and pilot workload, hence good fidelity.

The SFR scale builds on this approach by further quantifying differences in pilot task performance and amount of adaptation, defined as the differences in control strategy, compensation, available cueing or pilot workload between FS and RWS. This approach was also heavily used in the RoCS project, which updated the SFR scale to be appropriate for certification use cases [19]. The SFR is also mapped against a 10-point scale which is further classified into four fidelity 'levels' as defined in Table 3. The combination of techniques above is recommended because, while all have been shown to be useful, none have been demonstrated as a guarantee of sufficient fidelity in isolation.

Table 3: Simulation Fidelity Rating scale fidelity level definitions [21]

Level	Description
1	**Simulation fit for purpose:** Fidelity considered sufficient for full credit against a selected ACR.
2	**Simulation fidelity warrants improvement:** Fidelity considered sufficient for partial credit (SFR 3-4) or critical point analysis (SFR 5-6) against a selected ACR depending on rating.
3/4	**Simulation not fit for purpose**

To support assessment using the proposed metrics, a range of RWS data is required, which is routinely captured in initial qualification of a military rotorcraft against Def. Stan. 00-970 Part 7. This includes trim states, control step and sweep responses in a range of different mass and environmental conditions. Comparison of this data set with M&S equivalents is regarded as the basis of 'V&V for specific M&S' (MECC 3). The verification element must also be addressed to ensure the FSM and FS are implemented as intended via code and solution verification. Both elements can be quantified via the NASA-STD-7009B verification factor.

RA 5812 also mandates uncertainty characterisation and sensitivity analysis be performed to quantify the possible variance in the M&S outputs (MECCs 4 and 5). This approach is described in detail in the RoCS guidance, and demonstrated well in Ref. [28], where input parameter uncertainty intervals are used to drive Morris one-at-a-time and variance-based decomposition analysis on ADS-33E-PRF HQ metrics and aircraft frequency response against MUAD bounds. Both measures have also been identified as compliance metrics for SAI M&S, so this method is well suited. Using the Ref. [28] approach, it can be found whether input uncertainties may cause the expected M&S output to cross fidelity bounds. The RoCS guidance also proposes a way of quantifying this possibility using confidence ratios: the ratio of uncertainty magnitude to distance from a performance or fidelity boundary. Requirements on confidence ratio are mapped to the influence/predictability matrix concept, with higher confidence required for cases with higher influence or predictability, in a similar way to the RA 5812 criticality matrix. As such, this approach is also recommended here to provide requirements on maximum uncertainty. A more qualitative measure of uncertainty characterisation is provided by NASA-STD-7009B to scope the application of methods described above, which is recommended for compliance with MECC 4.

The NASA-STD-7009B M&S results robustness factor is also useful for quantifying the level of sensitivity analysis performed, which while related, is distinct from uncertainty characterisation. A particular metric may be very sensitive to an input parameter, but the uncertainty in it may be low enough to limit potential impact, e.g. rotor radius. Hence, both should be assessed independently, with sensitivity analysis often informing uncertainty characterisation.

Table 4: Proposed compliance standards and metrics to satisfy the RA 5812 technical MECCs for flight simulation model and flight simulator components of framework

MECC	Proposed Compliance Standards/Metrics
1.	• NASA-STD-7009B M&S data pedigree factor
2.	FSM compliance metrics: • CS-FSTD(H) performance and handling qualities tests • ADS-33E-PRF hover & low-speed HQ metrics with 10% fidelity bound • Maximum Unnoticeable Added Dynamics bounds FS compliance metrics: • Cooper-Harper HQR scale • Simulation Fidelity Rating scale
3.	FS/FSM verification: • NASA-STD-7009B M&S verification factor FSM validation: • RWS trim states, control step responses, control sweep responses in all axes FS validation: • ADS-33E-PRF MTE HQRs and performance data • Simulation fidelity ratings
4.	• NASA-STD-7009B M&S uncertainty characterization factor • RoCS confidence ratios
5.	• NASA-STD-7009B M&S results robustness factor

The proposed metrics and methods of compliance with the RA 5812 technical MECCs for the FS and FSM are collated in Table 4. The paper will now describe development of exemplar models then a fidelity assessment of the models using the metrics above. Note that values of NASA-STD-7009B factors will not be reported in this paper.

3.2 FSM & FS Development

For the purposes of the RCAT project and initial assessment of digital SA-R framework, an existing FSM of the AW159 Wildcat (Figure 4) was provided to UoL by LH, as an exemplar aircraft for assessment and integration into UoL's HELIFLIGHT-R FS [29]. The FSM is a non-linear flight dynamics model developed by LH, featuring coupled rotor-airframe equations of motion and independent aerodynamic models of the main rotor, tail rotor, fuselage and empennage surfaces, with additional propulsion and flight control systems models. The flight model also integrates with the Ship Air/Interface Framework (SAIF) simulation tool developed by SEA Ltd. [30] for the UK MoD. The model can be run in an offline mode via a MATLAB/Simulink interface, or via a real-time scenario manager for piloted simulation. No development of the FSM has taken place during the initial phases of the RCAT project to date, so all assessments through the framework have been carried out with the FSM in its 'as delivered' state. Due to the sensitive nature of any AS-related data, any numerical results reported here have been normalised and obfuscated. Units of any quantities plotted are intentionally omitted.

Figure 4: Royal Navy AW159 Wildcat Helicopter [31]

HELIFLIGHT-R (Figure 5) is a reconfigurable simulator for flight dynamics, control, handling qualities and simulation fidelity research. It features a 6 degree-of-freedom motion platform, a wide field-of-view 4-channel projection dome and 4-axis active control loading [29]. HELIFLIGHT-R is a generic simulator used to represent a wide range of fixed- and rotary-wing platforms, and as such presented several functional fidelity deficiencies when operating as an AW159 Wildcat. Some of these deficiencies became apparent during early project testing and renovations were performed for continuing simulator trials.

Figure 5: The HELIFLIGHT-R simulator at the University of Liverpool

3.3 FSM Fidelity Assessment

The exemplar aircraft has undergone an initial fidelity assessment using the proposed compliance metrics of Table 4. The FSM was provided as a black-box entity by LH, so the values of model parameters were not accessible for assessment against MECC 1, i.e. data and input V&V and pedigree. This arrangement also made verification of FSM code or solutions unfeasible; these activities are planned to be performed by LH in future phases of work.

A limited set of flight test data, drawn from initial qualification of the AW159 was used as reference for validation. This data set was captured with the intention of supporting qualification of training simulators, so some desired data for HQ and MUAD analysis was not available. Frequency sweep and varying magnitude control steps were notably absent, as these are not assessed in CS-FSTD(H). This precluded MUAD and restricted HQ analysis. Sourcing of further data is underway to support future phases of work. However, assessment of the model against the available data using CS-FSTD(H) and ADS-33E-PRF requirements is reported on here to demonstrate the process applied thus far.

Full qualification against CS-FSTD(H) was beyond the scope of this initial work and would also apply requirements that would not be relevant to this use case; SHOL determination is almost exclusively performed at hover and low-speed conditions, so high speed analysis is of limited utility. Key results on aircraft trim states and dynamic longitudinal control response are included to highlight fidelity issues discovered. Figure 6 shows some of the aircraft trim states across the hover and low forward speed envelope for both the RWS and FSM.

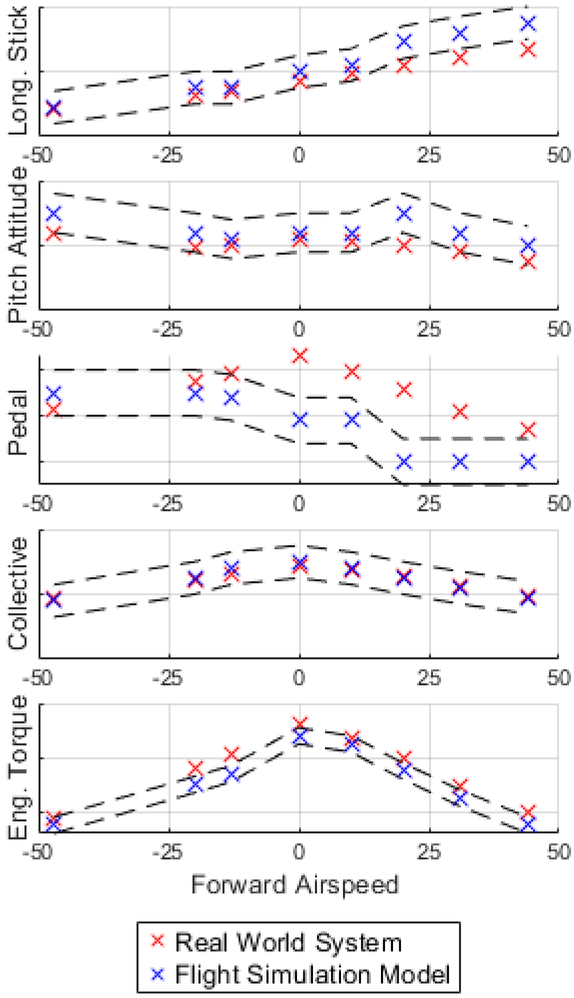

Figure 6: AW159 FSM trim states across hover and low forward/aft speed, plotted against equivalent RWS flight test trim conditions, with CS-FSTD(H) bounds applied.

Longitudinal stick position and pitch angle migrate out of acceptable range with higher forward speed, which is a regime the aircraft will likely operate in during SHOL assessments. Trim pedal position also migrates out of acceptable bounds with increasing forward speed. Pedal margin inaccuracy is of particular concern, as this can often be a limiting factor in determining SHOL. Lateral states (not shown) and collective position match flight test well, but engine torque is not compliant, if only marginally. All issues warrant further investigation and corresponding development of the FSM to improve match.

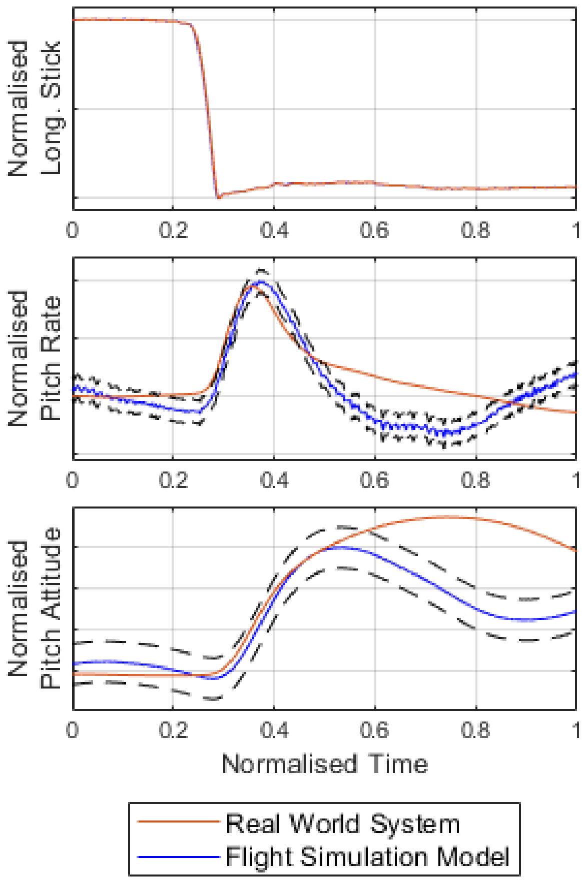

Figure 7: AW159 FSM response to a step input in longitudinal stick from hover, plotted against equivalent RWS flight test response, with FSTD(H) bounds applied.

The Wildcat's dynamic response to a step input in longitudinal stick is graphed in Figure 7. The FSM's initial peak in pitch rate response matches flight test well, but exhibits significantly higher damping over the medium term, resulting in a greater change in pitch angle for the FSM under the same applied input. Hence, neither pitch rate nor angle remain within CS-FSTD(H) 10% fidelity bounds over a medium duration input. CS-FSTD(H) does not place numeric bounds on modelling of cross-couplings but does require that expected couplings act in the correct direction and magnitude. For the coupled roll response to this input, direction of roll displacement was correct, but attenuated compared to flight test. For the inverse coupling (pitch due to roll), the coupling was absent.

As discussed in the rationale, additional HQ analysis was performed to address some of the perceived gaps in the CS-FSTD(H) requirements, and capture fidelity of more pilot-relevant qualities of the aircraft. A selection of hover and low-speed HQ requirements from ADS-33E-PRF were analysed using desktop simulation and compared against flight test data, listed in Table 5. The listed HQ requirements are those deemed relevant to the typical SHOL flying tasks, but appropriate RWS data was only available to characterise a relatively small number of them. The HQ metric values are not included due to the sensitive nature of the data, but percentage difference between the RWS metric value are given and highlighted in accordance with the fidelity bounds from Ref. [24]: green within 10%, red beyond 10%. All tests were performed at nominal mass and environmental conditions, trimmed at hover in nil wind.

Table 5: Comparison of AW159 RWS and FSM through ADS-33E-PRF handling qualities metrics

ADS-33E-PRF Req.	**Description**	**RWS/FSM % Difference**
3.3.2.1	Short term response to pitch/roll inputs (bandwidth)	N/A
3.3.2.3.1	Mid-term response to pitch/roll inputs	N/A
3.3.3	Moderate amplitude pitch attitude quickness	26.5%
3.3.3	Moderate amplitude roll attitude quickness	1.4%
3.3.4	Large amplitude pitch/roll attitude changes	N/A
3.3.5.1	Short term response to yaw control inputs	N/A
3.3.5.2.1	Mid-term response to yaw inputs	N/A
3.3.9.1	Yaw due to collective cross coupling	22.24%
3.3.9.2	Pitch due to roll coupling	66.7%
3.3.9.2	Roll due to pitch coupling	73%
3.3.10.1	Height response characteristics	N/A
3.3.10.2	Torque response	N/A
3.3.10.3	Vertical axis control power	31.7%

Roll qualities are represented well and fall within the 10% fidelity bounds, but pitch response does not provide adequate match, which is consistent with findings of the CS-FSTD(H) analysis. Cross couplings and vertical axis control power also do not fall within the required level 1 fidelity bound of 10%, or the level 2 bound of 20%. Deficiency in cross-coupling, particularly roll from pitch was also noted in CS-FSTD(H) analysis.

Ideally, these issues would be resolved before continuing to piloted simulation assessments, but further development of the FSM was not possible during the project timeline. However, modifications to fuselage aerodynamic modelling, main rotor wake, and tail rotor interference models are planned for further phases of the project to address these deficiencies. Full analysis of the suggested requirements is also preferable at a wider variety of flight conditions, covering mass, centre of gravity, wind and airspeed variations.

Uncertainty characterisation and sensitivity analysis is also required on the FSM by MECCs 4 and 5, respectively. However, the inaccessibility of parameters in the black-box model precluded addressing these factors. An approach to future compliance with these requirements has been agreed with LH, inspired by the processes reported in Ref. [28].

3.4 FS Fidelity Assessment

The inputs to the FS can be viewed as a combination of the FSM, and the physical qualities of the aircraft that are to be replicated. This includes cockpit field-of-view, control mechanical characteristics, flying control geometry, instrument panel geometry and many others. Much of this information was provided by LH via manufacturer design drawings, digital 3D models, and reports, but was further verified by physical measurements of the aircraft performed by FS&T. As such, the pedigree of inputs to physical design of the FS was high, with good verification performed. Integration of the FSM into the FS was also verified by performing step control inputs 'online' in the FS, and repeating the same tests using the offline FSM and comparing resulting aircraft states for equivalence.

To validate the FS (and also by extension the FSM), a piloted simulation trial was performed. Seven hover and low-speed ADS-33E-PRF MTEs were selected for testing in the HELIFLIGHT-R. The MTEs were selected for their relevance to the flying tasks required to perform the port forward-facing approach and landing described in Section 1. Precision hover and depart/abort manoeuvres were used to exercise similar handling qualities to the first two phases of the landing: deceleration to hover and hover alongside. Sidestep and slalom MTEs approximated the transition across the deck, and a vertical manoeuvre served as an analogue for the final vertical descent and landing. Pirouette and hover turn MTEs were also used to exercise directional HQs that are generally relevant in hover and low-speed flight. The MTEs were performed using test courses defined in ADS-33E using cones and hoverboards. Three examples of the test courses used for the MTEs are given in Figure 8.

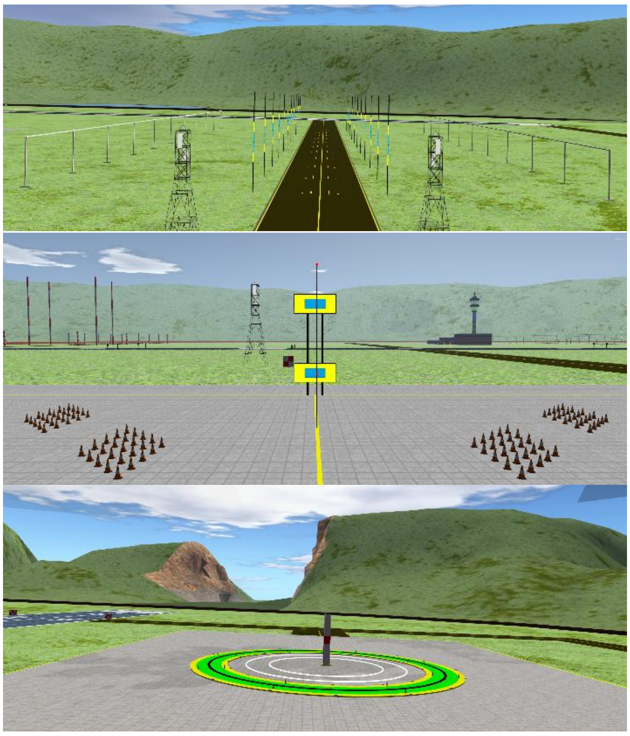

Figure 8: HELIFLIGHT-R visual cueing environment for ADS-33E-PRF MTEs: depart/abort (top), vertical manoeuvre (middle), pirouette (bottom)

Each MTE was flown by three TPs and rated using HQR and SFR scales. Equivalent HQRs from the RWS were used as referent data for validation, and the resulting differences between average HQRs captured in the FS and RWS are given in Figure 9, along with average SFRs awarded by the TPs for each MTE flown. Accompanying error bars signify the range of ratings given by the TPs.

Average HQRs matched exactly for the depart/abort, prevision hover and slalom MTEs, and were within 1 rating for the hover turn and pirouette manoeuvres. Across the manoeuvres, pilots generally reported FS response was a good representation of the AW159 in most axes, but a significant level of compensation was required on the collective control that would not be expected in the RWS. Pilot perception was that this deficiency was due to excessive sensitivity to collective inputs. This hypothesis is supported by the FSM analysis, which found significantly higher vertical control power when compared to the RWS. This adaptation contributed to level 2 SFRs across all MTEs, with deficient vestibular motion cues and cockpit field of view inaccuracies cited as other causes by the TPs.

The sidestep and vertical manoeuvre HQRs matched significantly more poorly. The sidestep was evaluated with a much higher HQR due to pilot inability to maintain altitude performance standards. The vertical manoeuvre was awarded a much lower HQR than the RWS on average. No commentary was available from RWS testing to justify the difference, but it is hypothesised that increased vertical control power in the FSM makes the task easier.

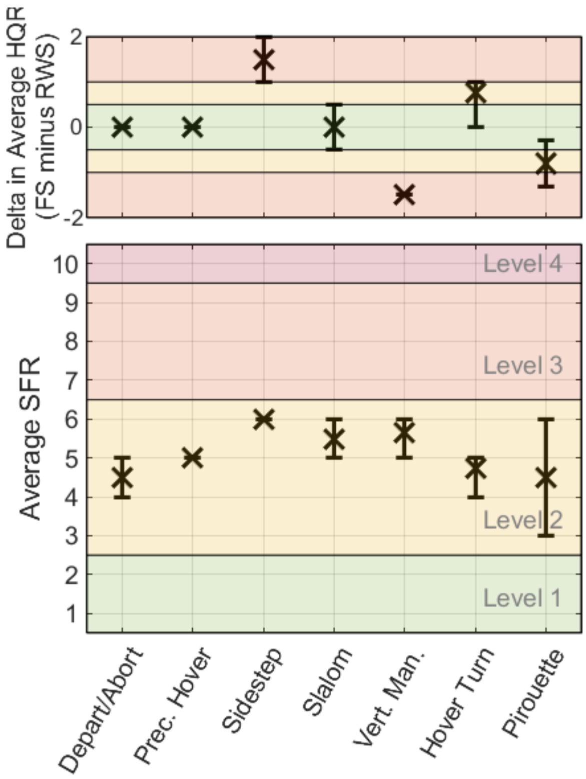

Figure 9: Difference in average HQR between FS and RWS, and average SFR across tested ADS-33E-PRF MTEs

All average SFRs fell within level 2 and were above rating 4, indicating that the simulator warrants improvement before full or partial credit against a certification requirement could be claimed. In an effort to improve the SFRs for subsequent flight testing, further renovations to the HELIFLIGHT-R were then made to improve flying control representation and further tune vestibular motion, vibration and audio cues.

Uncertainty characterisation is a somewhat nebulous concept when discussing piloted simulation, since the emergent nature of piloting makes FSM/FS uncertainties difficult to isolate. The accepted practice of averaging TP ratings across three pilots provides an approach to quantifying uncertainty in these experimental measurements through recording of the range of ratings with the average, as denoted by the error bars in Figure 9. The uncertainty in most of the captured ratings is low and generally spans only one rating. However, the uncertainty in the pirouette rating is noticeably higher at ±1.5, so should be treated with caution. Use of more pilots could enable more informative metrics like standard deviation of the rating but comes with cost implications. An extension of the process using to quantify uncertainties in the FSM could be applied to propagate FSM input uncertainties and test for effect on the FS compliance metrics, but this would create a very wide test matrix for simulator testing, and it is unclear whether this level of uncertainty characterisation is necessary. This approach was not possible with the initial black-box FSM regardless, but regulator input is sought on this matter to scope future work.

A critical sensitivity for simulators with vestibular cueing systems is the tuning of motion platform gains. Motion cues were highlighted as a deficiency of the HELIFLIGHT-R in some MTEs, and limited tuning of heave axis gains was performed during the trial to address the most obvious deficiencies. These changes did improve both HQRs and SFRs when they were applied. Further testing is planned to assess these sensitivities and optimise motion tuning parameters. Sensitivity in other simulator design parameters is very difficult to assess without significant simulator redesign that can be prohibitively expensive. Like uncertainty characterisation, sensitivity analysis of FSM input parameters would carry a high testing burden that may not be necessary, and discussion is needed to inform further efforts.

3.5 FS/FSM Summary

An initial fidelity assessment of an AW159 Wildcat AS model, provided by LH, has been completed. The model was assessed in isolation via offline predictive analysis, and through perceptual fidelity assessment in UoL's HELIFLIGHT-R simulator. Pedigree of the inputs to the FSM is unclear, as the model was provided in a black box format. However, inputs to the FS are generally traceable and have been verified by UoL. Due to model access restrictions, code and solution verification, uncertainty characterisation and sensitivity analysis could not be performed.

A validation assessment of the FSM has been conducted by comparison of RWS data against the model using CS-FSTD(H) and ADS-33E-based fidelity standards. Results show good agreement of lateral performance and handling qualities metrics but minor deficiencies in the longitudinal and directional axes, and more significant deficiencies in the heave axis. Additional validation of HQRs awarded for ADS-33E MTEs was conducted, supporting the conclusions of offline analysis. Supplementary SFR ratings also indicate the AS model sits within fidelity level 2. Further development of the AS model is recommended to address the identified deficiencies in the FSM and to enable input V&V, uncertainty characterisation and sensitivity analysis in accordance with RA 5812.

4 Ship System Model

The Ship System Model (SSM) is of equal importance to the AS model in digital SHOL determination, but its definition is more limited in scope. Here, the SS term refers specifically to the dynamic factors associated with the ship that affect helicopter operations. These factors include the turbulent air flow in the lee of the ship superstructure and over the ship's flight deck (known as the airwake), along with ship motions caused by a rough seaway. Other elements of the ship unrelated to AS operations are omitted.

4.1 Assessment Rationale and Methodology

Any assessment of the SSM must again satisfy the RA 5812 MECCs described in Section 1.2 if it is to be used in SA-R development. Like the AS, there is no definitive fidelity standard that covers SS models, so a combination of sources must be used to provide a basis for fidelity assessment. NASA-STD-7009B can again be used to cover MECC 1 (data and input V&V), but defining mechanisms for measuring compliance presents some significant challenges for this component of the SA-R framework. No sources have been found that establish fidelity bounds on the ship airwake, the most prominent element of the SS model. The ship airwake is typically modelled as a four-dimensional field of time varying air-velocity components, generated using a CFD model that captures the unsteady flow structures present in the wake of the ship.

CFD modelling of ship airwakes is a well-established approach, with standards such as ASME V&V 20-2009 outlining verification and validation processes for CFD more broadly. However, like NASA-STD-7009B, they do not define fidelity bounds. Ref. [32], for example, established mean velocity and turbulence intensity as useful metrics in ship CFD validation, but did not explore potential impact of variations in those metrics on pilot and aircraft performance during SHOL determination. If differences between the modelled and real-world environments are small, then discrepancies may go unnoticed by pilots operating in the simulated environment. However, if M&S fidelity is poor, a resultant predicted SHOL may be significantly compromised. As what constitutes a significant difference between M&S and referent data is currently unclear, the authors have designed and carried out a piloted simulation trial to establish new airwake fidelity bounds. This was achieved by artificially modifying airwake mean velocity and turbulence and measuring variations in pilot workload and task performance during a simulated ship deck landing. The investigation and suggested bounds are reported on further in Section 4.3.

After airwake fidelity bounds were established, they were used to validate M&S against experimental measurements of air flow over the chosen SS, the Royal Navy's Type 23 frigate. Experimental measurements were collected using FS&T's large recirculating water tunnel, and from anemometer data captured during at-sea trials of the Type 23. These data sets provide for the specific validation requirements of MECC 3. The NASA-STD-7009B verification factor has again been used to quantify efforts to verify code and solutions produced.

MECCs 4 and 5 can also be assessed using the NASA uncertainty characterisation factors and results robustness factors for the SSM. ASME V&V 20-2009 provides methodologies for quantifying uncertainty in CFD analysis that can be usefully applied in this situation. These uncertainties can be highly dependent on the applied solution discretisation approach (spatial and temporal), so grid convergence studies are recommended to check that solutions are independent of grid sizing. These studies can be assessed using the ASME grid convergence index as a measure of uncertainty minimisation. Input uncertainty can be propagated via Monte Carlo analysis, but due to the high computational cost of running ship CFD calculations, this approach has limited utility and must be applied sparingly. Latin hypercube sampling is advocated by ASME V&V 20-2009 to reduce the scope of Monte Carlo analysis efficiently. Uncertainties in RWS measurements of the SS can also be high, so must also be considered for SSM validation. The proposed compliance metrics for the SSM are collected in Table 6, with development of the new airwake fidelity bounds and validation carried out in the following sections.

Table 6: Proposed compliance standards and metrics to satisfy the RA 5812 technical MECCs for ship system model component of framework

MECC	Proposed Compliance Standards/Metrics
1.	• NASA-STD-7009B M&S data pedigree factor
2.	• ASME V&V 20-2009 • Airwake turbulence intensity and mean velocity fields
3.	SSM verification: • NASA-STD-7009B M&S verification factor SSM validation: • Recirculating water tunnel model testing • RWS Air Flow Air Pattern data
4.	• NASA-STD-7009B M&S uncertainty characterization factor • ASME V&V 20-2009 grid convergence index metric and Latin hypercube sampling method
5.	• NASA-STD-7009B M&S results robustness factor

4.2 SSM Development

In this section, the approaches to modelling both the ship airwake and the ship's motions due to sea state are presented. There are several inputs to the SSM model, for both ship airwake and motion, and an evaluation of the fidelity of these inputs is discussed later in Section 4.4.

4.2.1 Ship Motion

SS motion is considered important in the simulation environment as it has the potential to significantly impact pilot workload during embarked operations. Furthermore, the pilot must land to the moving deck so the fidelity of the SS motions should be such that the simulation feels realistic. To develop realistic SS motion profiles, there are a few options to consider. If available, RWS ship motion data can be recorded and implemented in simulation; however, this may be limited to a few combinations of conditions (i.e., different sea states, wave headings etc.). Alternatively, the SS motions can be simulated for various sea states, e.g., using tools such as ShipMo3D [33]. In the present study, the ship motions were supplied with the AS model provided by LH.

A range of sea states were used for this study, between SS3 and SS6, selected to match the embarked trials where appropriate, or selected to best match the desired wind speed considering what would be a realistic scenario. The definitions of the scale used to define sea state is given in NATO Standardised Wave and Wind Environments and Shipboard Reporting of Sea Conditions [34].

4.2.2 Ship Airwake

The CFD-generated airwakes for the Type 23 SSM were computed by UoL and are reported on in Ref. [35]. These airwakes were computed using the commercially available CFD solver, ANSYS Fluent, employing time-accurate Delayed-Detached Eddy Simulation (DDES). This CFD approach has been validated on several occasions [36], [37] and has been shown to be suitable for modelling ship airwake for the purpose of integrating with flight simulation models [32].

There are several key steps involved in the ship airwake numerical modelling process, as illustrated in Figure 10, which include defining the solution domain and boundary conditions, generating a computational mesh (i.e., spatial discretisation of the solution domain), generating CFD solutions (steady and unsteady), and processing the sampled data for the required application. Considering each of the steps outlined in Figure 10:

- **Step 1:** It is important the solution domain (i.e., the solution boundaries and 3D ship model) and boundary conditions accurately represent the

RWS, including using suitably realistic ship geometry and atmospheric wind conditions.

- **Step 2:** For the CFD calculations, a viscous hybrid approach to generating a computational grid was applied, as employed previously by Ref. [38], whereby prismatic layers are used in near-wall regions to adequately model the boundary layer, and tetrahedral volumetric cells are used in the free-shear flow regions. When generating a computational grid, it is important that it meets specific criteria to generate accurate solutions, and which are often dependent on the applied CFD approach. Therefore, a first attempt at a grid is typically generated and then a solution computed (i.e., **Step 3a**), typically using a steady Reynolds-Averaged Navier Stokes (RANS) turbulence model so that the relevant checks can be carried out. In this instance, these checks include assessing spatial and temporal resolution of relevant turbulence scales (and ensuring the resolution is suitable for the DDES approach), as well as suitable resolution in the near-wall regions. To pass these checks, refinements of the grid in appropriate regions are often required.

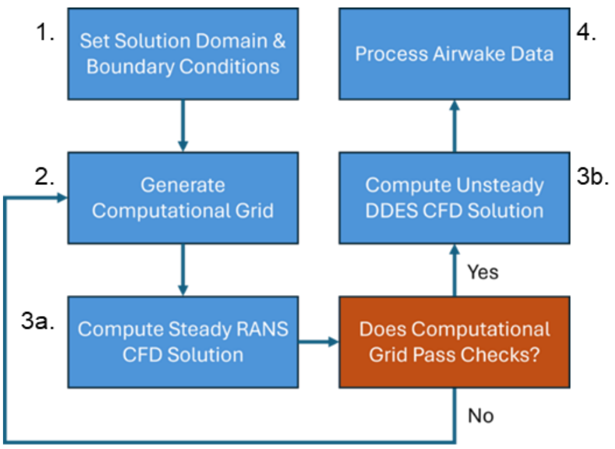

Figure 10: Flow diagram illustrating an overview of the process for generating a ship airwake with CFD.

- **Step 3b:** After the computational grid has passed the appropriate checks, the unsteady DDES solution is computed, where initial conditions are set to the steady RANS solution. It is also important to match the solver settings to the physics of the problem, and to optimize numerical settings and scheme selection for solution accuracy; a further discussion on this subject is made in Ref. [38]. Prior to data sampling, a solution settling time is required so that the air flow can reach a quasi-steady state; this period is typically set to around two-and-a-half flow-passes of the ship, e.g., Ref. [38] .
- **Step 4:** Finally, the airwake data that is exported during unsteady CFD computations is processed in preparation for integrations with the FSM.

Following the approach outlined above, several airwakes were computed around the azimuth of relative wind directions, using a 40 kts reference WOD speed. The airwakes can be produced at one WOD speed per azimuth direction and then scaled in the simulation to different wind speeds (using Reynolds and Strouhal scaling as demonstrated in Ref. [12]), hence reducing the total number of required CFD simulations. These computed WOD conditions were chosen to capture the typical features observed in a SHOL for a frigate/destroyer, and a full list is provided in Table 7. Winds approaching from the port side are typically described as red (R), and green (G) from the starboard side.

Table 7: WOD conditions for the computed ship airwakes.

	WOD Azimuth (°)	**WOD Speed**
Head winds	0	40 kts
Green winds	15, 30, 45, 60, 90, 135	40 kts
Red winds	15, 30, 45, 60, 90, 135	40 kts
Stern winds	180	40 kts

4.3 Determination of Airwake Fidelity Bounds

A piloted simulator trial was performed with the aim of assessing the impact of airwake variations on pilot workload and task performance. To determine suitable airwake fidelity bounds for integration with FS, it is important to understand the effect that variations in the airwake have on the pilot and helicopter.

4.3.1 e-CETI Ship Airwake Model

To create artificial variations within the SSM airwake, FS&T utilised the enhanced-Control Equivalent Turbulence Input (e-CETI) model developed in Ref. [9]. Although FS&T have the capability to integrate full unsteady airwakes with the AS model, the e-CETI model was used to facilitate a flexible approach to creating airwake variants, with direct control over the compliance metrics defined in Table 6. The e-CETI turbulence model is characterised by a transfer function for each of the four control axes, $[\delta_{Lat}, \delta_{Long}, \delta_{Coll}, \delta_{Ped}]$. These functions are driven by a white noise generator (w_n), and are parameterised by freestream wind velocity (U_∞), aircraft main and tail rotor radii (R_m and R_t), and the standard deviation of the component airwake velocities $[\sigma_u, \sigma_v, \sigma_w]$. The transfer functions are given in Equations (1) to (4) below:

$$\text{(1)} \quad \frac{\delta_{Lat}}{w_n} = 0.837\sigma_w(t)^{-0.6265}\sqrt{\frac{\sigma_w^2 U_\infty}{\pi R_m}}\left[\frac{1}{s + 2\frac{U_\infty}{R_m}}\right]$$

$$\text{(2)} \quad \frac{\delta_{Long}}{w_n} = 1.702\sigma_w(t)^{-0.6265}\sqrt{\frac{\sigma_w^2 U_\infty}{\pi R_m}}\left[\frac{1}{s + 2\frac{U_\infty}{R_m}}\right]$$

$$\text{(3)} \quad \frac{\delta_{Coll}}{w_n} = 0.1486\sigma_w(t)^{-0.7069}\sqrt{\frac{3\sigma_w^2 U_\infty}{\pi R_m}} \times \dots \left[\frac{s + 33.91\left(\frac{U\infty}{R_M}\right)}{\left(s + 1.46\frac{U_\infty}{R_m}\right)\left(s + 9.45\left(\frac{U\infty}{R_m}\right)\right)}\right]$$

$$\text{(4)} \quad \frac{\delta_{Ped}}{w_n} = 1.573\sigma_v(t)^{-0.6265}\sqrt{\frac{\sigma_v^2 U_\infty}{\pi R_t}}\left[\frac{1}{s + \frac{U_\infty}{R_m}}\right]$$

The mean airwake velocity field was mapped onto the AS model through Airload Computation Points (ACPs), positioned across its aerodynamic components. The $[u, v, w]$ airwake velocity components at each ACP, along with the standard deviations of the velocity components $[\sigma_u, \sigma_v, \sigma_w]$ at the AS model centre, were obtained from spatial lookup tables. The mean and standard deviation velocity lookup tables were computed from the unsteady CFD-generated airwakes of the Type 23 SSM, collapsing the three 4-dimensional matrices of the unsteady airwake components into six 3-dimensional matrices that were easier to modify and scale.

The airwake turbulence intensity (TI, derived using $\sigma_u, \sigma_v, \sigma_w$ as shown Eqn. (5)) was modified simply by multiplying the velocity component standard deviations (that were integrated with the e-CETI model) by the desired scale factor, SF_{TI}. Scaling the component standard deviations consequently scaled the total TI by the same factor. The equation for modifying the TI is given in Eqn. (6).

$$\text{(5)} \quad TI = \frac{\sqrt{\frac{1}{3}(\sigma_u^2 + \sigma_v^2 + \sigma_w^2)}}{U_\infty}$$

$$\text{(6)} \quad \begin{bmatrix}\sigma_u \\ \sigma_v \\ \sigma_w\end{bmatrix}_{modified} = SF_{TI} \cdot \begin{bmatrix}\sigma_u \\ \sigma_v \\ \sigma_w\end{bmatrix}_{acutal}$$

Applying a scale factor to the mean velocity field (SF_{vel}) was complicated by the necessity that regions of freestream flow were not affected by scaling. For this reason, it was not suitable to simply multiply all velocity components by a scale factor, or to add an offset to the entire mean velocity field. Therefore, the approach taken was to scale the difference between the mean airwake velocity from the freestream WOD (referred to as the velocity perturbation), which resulted in no modification to the freestream regions, whereas areas in the lee of the ship were scaled. The equation used to scale the airwake mean velocity field is given in Eqn. (7).

$$\text{(7)} \quad \begin{bmatrix}\bar{u} \\ \bar{v} \\ \bar{w}\end{bmatrix}_{modified} = SF_{vel} \cdot \left(\begin{bmatrix}\bar{u} \\ \bar{v} \\ \bar{w}\end{bmatrix}_{acutal} - \begin{bmatrix}u_\infty \\ v_\infty \\ w_\infty\end{bmatrix}\right)$$

4.3.2 Trial Aircraft and Flight Simulator

The aircraft simulation model used for the investigation was the National Research Council of Canada's Bell 412 advanced systems research aircraft, which has capabilities for variable handling qualities [39]. The model was developed by FS&T in FLIGHTLAB, a state-of-the-art, finite element, selective fidelity modelling and analysis software package [40]. The Bell 412 model has seen extensive validation against RWS data in Refs. [41] and [42]. It was implemented in the HELIFLIGHT-R simulator, described in Section 3.2. Due to its similar rotor diameter and mass, the 412 was selected as an analogue for the AW159 in this trial, which could not support integration of the e-CETI airwake. The handling qualities of the 412 were also modified for improved attitude quickness, close to that of the AW159. It was reasoned that the physical similarities between the two aircraft should equate to similarity in response to equivalent ship airwakes, and hence any resulting fidelity bounds would be applicable to both aircraft. However, further work will investigate the sensitivity of turbulence and velocity bounds to airframe properties.

4.3.3 Trial Results and Airwake Fidelity Bounds

Using the UK Royal Navy port forward-facing approach, multiple ship deck landings were performed to the Type 23 frigate with the Bell 412 AS model. The approach and landing task was subdivided into four MTEs to allow for assessment of pilot workload at each phase of the task. As illustrated in Figure 1, the four MTEs were: approach to station keeping, lateral translation across deck, hover above landing spot, and landing. Pilot workload was assessed at each phase using the Bedford Workload Rating (BWR) scale [43], and pilot effort was assessed over the series of MTEs using DIPES. The MTEs were flown continuously without breaking between each phase of the overall recovery task. Test points were performed by at least two TPs wherever possible. The WOD conditions and scale factors that were investigated during this simulator trial are given in Table 8.

Table 8: Wind-over-deck conditions investigated during airwake fidelity bounds study

Wind Direction	Wind Speed	SF_{vel}	SF_{TI}
HWD	30 kts	0.8, 0.9, 1.0, 1.1, 1.2, 1.4	0.8, 0.9, 1.0, 1.1, 1.2
	40 kts	0.8, 0.9, 1.0, 1.1, 1.2, 1.4	0.8, 0.9, 1.0, 1.1, 1.2
G30	20 kts	0.8, 0.9, 1.0, 1.1, 1.2, 1.4	0.8, 0.9, 1.0, 1.1, 1.2
	30 kts	0.8, 0.9, 1.0, 1.1, 1.2, 1.4	0.8, 0.9, 1.0, 1.1, 1.2

In the analysis of the simulator trial results, the relationships between the pilot ratings and the airwake scale factors (for both mean velocity and TI) were correlated with linear trendlines, and a selection of the results are shown in Figure 11 and Figure 12. For this discussion, the G30 cases are considered due to the presence of interesting flow features, i.e., shear layers and a high degree of turbulence. BWR shown are for the lateral transition MTE (across deck), since this is where these flow characteristics are most prevalent.

Figure 11 shows the recorded DIPES and BWR values across the range of scale factors applied for mean velocity perturbation, for the G30 20 kts case. To reiterate, the scale vector is applied to the time-averaged velocity perturbations from freestream wind speed. Hence, the scale factor does not change the freestream wind speed, just the relative strength of the steady-state structures in the ships airwake. The results show that as the mean velocity scale factor increased, pilot workload did not change significantly, with only minor differences shown in the BWR. Similarly, there is no variation in DIPES suggesting no changes in SHOL would occur within the explored range of scale factors. However, it may be anticipated that a change in SHOL may still occur, for example, if the helicopter was closer to a performance limit, where a small change in local wind speed may result in a limit being reached. Based on the apparent lack of sensitivity to the tested variation, a 20% tolerance on mean velocity magnitude is proposed as an initial fidelity bound.

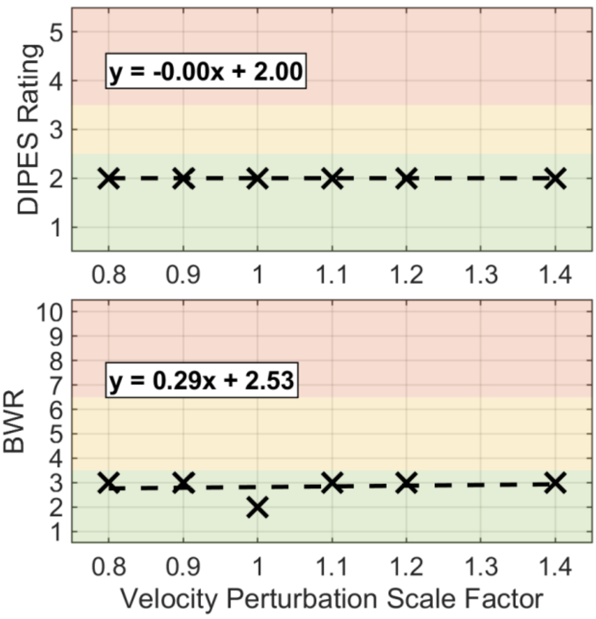

Figure 11: Pilot ratings for the Bell 412 in a G30 20 kts WOD, with varying e-CETI airwake velocity perturbation scale factor. DIPES ratings are for entire task, and BWR are for the lateral translation (across deck) MTE.

The ratings shown in Figure 12, for the G30 30 kts WOD condition, show a clear increase in BWR when increasing the TI scale factor. To determine the sensitivity of BWR to TI scale factor, the bounds for which a distinct change in BWR would occur were determined. These bounds were derived by using a line of best fit to calculate the change of TI scale factor required for a difference ±0.5 BWR. From this analysis, it is found that for ±0.5 BWR, the airwake TI must be accurate to within ±10% of the actual TI level. However, even though a clear change in BWR is observed in these results, there is no change in DIPES shown across the range of TI scale factor. This finding indicates that despite an increased BWR, the workload level is still tolerable for the tested condition (consistent with the BWR 2-4 given in the trial). As discussed for the mean velocity scale factor, if the helicopter were closer to performance limits, then a change in DIPES may still have occurred.

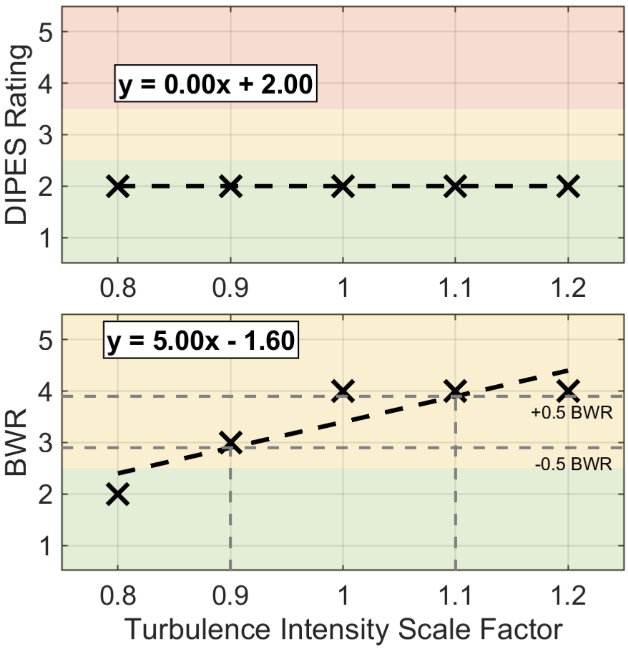

Figure 12: Pilot ratings for the Bell 412 in a G30 30 kts WOD, with varying e-CETI airwake TI scale factor. DIPES ratings are for entire task, and BWR are for the lateral translation (across deck) MTE.

4.4 SSM Fidelity Assessment

The characteristics of the SS model are strongly dependent on the geometry used in CFD and ship motion analysis, which is the primary input to this model. Geometry of the RWS is often simplified to omit small features that will have little practical effect on the airwake before generation of CFD meshes, which would require very fine resolution without these simplifications. However, there has been a reduction in the degree of simplification required for CFD since the airwakes were originally generated, and this could be improved on. It should also be noted that the geometry of the Type 23 itself has changed since the airwakes were computed, with large radar fences above the hangar removed. The geometry used in this investigation reflects the original configuration of the Type 23. There is high confidence in the geometry used and the experimental model was printed using the same 3D model as used in the CFD analysis..

Since the CFD analysis was performed using Ansys Fluent, a software package that has been verified against numerous standard cases [44], the codes of the SSM can also be considered verified. Setup of simulation and best practice for execution was verified independently by Frasier Nash Consultancy, with agreement on the geometry and associated simplifications.

The metrics and fidelity bounds developed in Section 4.3 have been applied to validate the SSM against referent data generated from scale model testing in FS&T's large recirculating water tunnel. The water tunnel features a working section of 3.8 m long by 1.4 m wide, with an adjustable floor allowing water depth of up 0.85 m, providing uniform inlet velocities from 1 m/s to 6 m/s. For this assessment, it was used as a 'wet wind tunnel', with a model of the Type 23 submerged in the working section as shown in Figure 13. Flow data was collected with the use of a Nortek Vectrino Plus Acoustic Doppler Velocimeter (ADV) probe, which was attached to a three-dimensional programmable traverse system mounted to the flume [32]. The traverse system allows for positional accuracy and repeatability for each chosen sampling point.

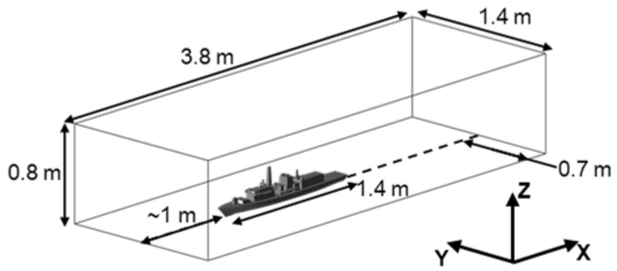

Figure 13: Schematic of the Type 23 model in the UoL large recirculating water tunnel working section.

While use of a water tunnel allows closer Reynold's number matching to that of a full-scale ship due to higher fluid density, there is still a significant difference between the two scenarios. Hence, to isolate potential Reynold's number effects on the solution, CFD analysis of the water channel was performed to provide a midpoint between experiment and the full-scale CFD to be used in simulator trials. Both full-scale and model-scale CFD results were extracted at the same locations as the experimental measurements to enable direct comparison. While the experimental measurements and corresponding CFD of the water tunnel have uniform inlets, the full-scale Type 23 SSM airwake had a velocity profile applied at the inlet to best represent at sea conditions.

Figure 14 shows the comparison of velocity magnitude of the flow between the three datasets at varying heights above the centre of the ship landing deck, plotted against the ±20% velocity magnitude bounds that were identified in simulator testing. These boundaries are applied against the water tunnel experimental result, which is regarded as the referent for this investigation. Both the full-scale and model-scale CFD results fall within the 20% bound from the experimental measurements, with full-scale CFD matching better than model-scale, surprisingly. The reason for the difference between model-scale CFD and experiment is unclear and will be further investigated in future work.

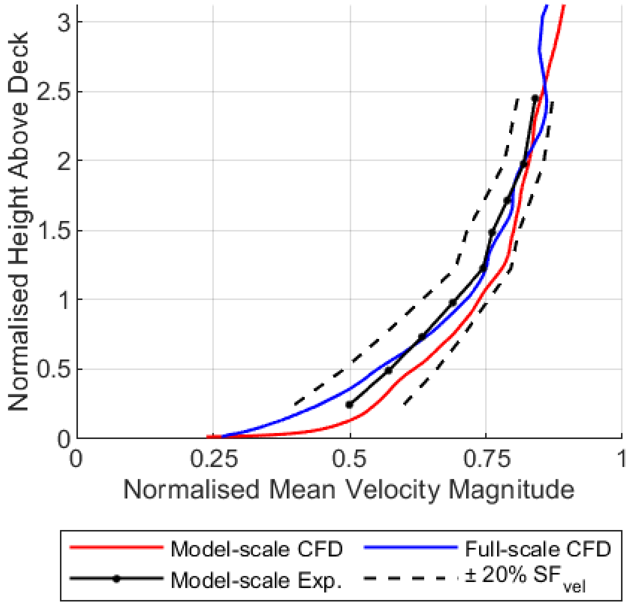

Figure 14: Comparison of mean velocity magnitude (normalised by freestream velocity) against height above deck (normalised by hangar height) between experimental and CFD results for a vertical profile over the flight deck. The derived mean velocity magnitude fidelity bounds applied to experiments.

This measurement was repeated at multiple spots across the ship landing deck and good agreement between experiment and full-scale CFD was found throughout for mean velocity in a headwind condition. Further experimental measurements are required to validate the SSM airwakes at varying wind directions.

Figure 15 shows the turbulence intensity for the v-component of velocity for the three sets of data. As a result of the how the ADV probe functions, only the turbulence intensity in the direction of the probe can be accurately determined. The data was collected with the ADV fitted with a sideways probe, providing the turbulence intensity in the v-component. It can be observed that the turbulence intensity measured by the probe was lower than that in the CFD. The maximum difference was between the experimental measurements and the scaled CFD with a value of 4.4% at hangar height. The agreement between the full scale CFD and the experimental measurements is closer with some values within ±1% turbulence compared to the experimental measurements, particularly around hangar height where a large portion of flying will take place.

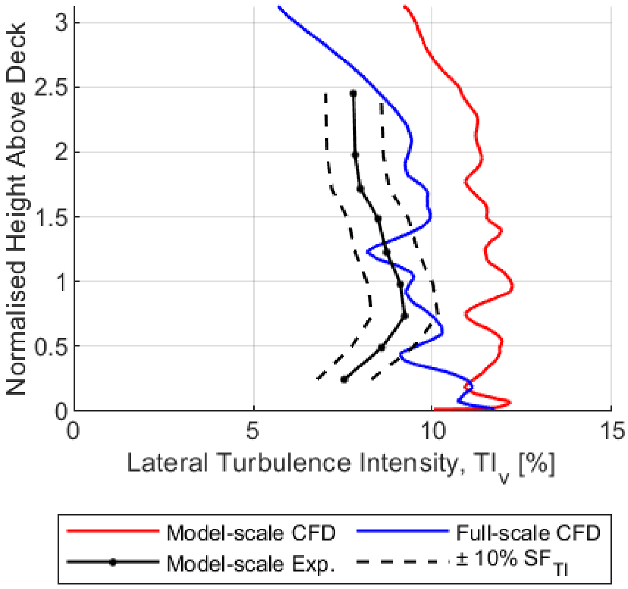

Figure 15: Comparison of lateral TI against height above deck (normalised by hangar height) between experimental and CFD results for a vertical profile over the flight deck. The derived TI fidelity bounds applied to experiments.

Per ASME V&V 20-2009, uncertainty in the experimental result should be quantified. Ref. [45] describes the uncertainty in the ADV probe measurements as a combination of steady-state bias and short-term random error. The former is the error that remains after long duartion time averaging, and is primarily driven by manufacturing defects. It is assessed in the product documentation as less than 1%. Short-term random errors are expected to cover a distribution around the bias error and so can be mitigated by time averaging. Since mean velocity measurements necessarily require time averaging, these short-term errors are not expected to affect the experimental results. The steady state bias may shift the experimental result by 1%, which is not large enough to render the full-scale CFD non-compliant.

Since turbulence intensity is a measure of unsteadiness in the flow, short-term errors in the measurements will not be averaged out. Uncertainty of turbulence measurements in the water tunnel has previously been assessed by measuring turbulence of undisturbed flow as described in Ref. [46]. That investigation concluded that uncertainty in the turbulence measurements was approximately 1%. However, quantification of experimental uncertainty is of limited use if uncertainty of the M&S is unknown. This uncertainty analysis will likely require recomputation of the CFD airwakes with a Monte Carlo approach, which has significant time and cost implications that were outside the scope of this project. However, ASME V&V 20-2009 does provide a mechanism for efficient construction of Monte Carlo analysis via the Latin hypercube sampling method for generating input parameter samples without requiring full-factorial analysis. Further work will apply this method to quantify uncertainty in the complex CFD wakes.

Sensitivity analysis can again be expensive to perform for CFD cases with lengthy computation times, but a variety of factors can affect solutions. This includes the geometry simplifications previously discussed, numerical parameters of the CFD, inlet conditions and boundary layer models. Modelling of additional physics should also be considered that may include integration of ship motion to CFD analysis, consideration of ship exhaust and unsteady inlet conditions. Many of these sensitivities have been previously explored by FS&T in Refs. Such as [47], [48] and found modest improvements in fidelity that typically do not justify increased computation times but were not assessed for the Type 23 specifically. Sensitivity to numerical parameters was assessed in model development (Section 4.2) via grid and timestep refinement.

4.5 SSM Summary

An initial fidelity assessment of the Type 23 SSM has been performed. Literature review highlighted a lack of applicable fidelity standards for ship airwakes, prompting a piloted simulation experiment to assess pilot sensitivity to varying airwake characteristics. Pilot workload ratings from the trial have been used to define preliminary fidelity bounds on airwake velocities and turbulence intensity.

The geometry and ship motion inputs to the SSM are of good pedigree and have been verified with independent partners, but the level of ship geometry simplification could be reduced with modern practices. Verified commercial software was used for CFD analysis, so the model is considered adequately verified. Validation of the CFD airwakes was performed against experimental measurements from a scale model of the Type 23 in UoL's large recirculating water tunnel. Mean velocity components over the ship show good agreement between experiment and CFD, within the newly defined fidelity bounds. However, turbulence intensity did not consistently meet the proposed standard. While uncertainty in the experimental measurements has been quantified, further analysis is required to assess sensitivity and uncertainty in the CFD analysis.

5 Integrated Air & Ship System Models

The integrated model is the combined AS and SS models, which can run in an offline or piloted mode, i.e. with or without the FS in the loop. It is the system ultimately used for determining a candidate SHOL.

5.1 Assessment Rationale and Methodology

Fidelity assessment of the integrated models presents a significant challenge as there is again no single applicable standard, and the ultimate aim of the framework is to enable SHOL prediction that informs, supplements, or eventually replaces embarked trials. Hence, integrated model testing will generally be performed in the absence of validation data. This is the primary driver behind the detailed assessment of the component AS and SS models, but some final assessment is important to ensure credibility of the integrated models.

The integrated model's only inputs are the two component models, so the first MECC can be assessed as an extension of the AS and SS models input, verification and validation factors. Metrics for compliance of M&S fidelity are somewhat difficult to define due to the emergent nature of SHOL testing, but the DIPES ratings that must be captured for compliance with Def. Stan. 00-970 are a useful measure and are here proposed as the primary validation metric. In the proposed framework, the integrated AS and SS models are first used in an offline mode for prediction of the SHOL. This approach is useful to limit the amount of piloted simulation required, and hence test pilot time investment. However, there are currently no methods that provide a DIPES rating based on offline analysis, so validation cannot be performed following offline analysis, only following piloted simulation. It is also suggested that the SFR scale is applied as a validation metric, as in FSM/FS validation. If assessment of the integrated model is performed before embarked test, it should be reassessed once data becomes available before submission as evidence for SA-R.

As before, NASA-STD-7009B uncertainty characterisation and results robustness factors can be used to show some level of compliance with MECCs 4 and 5, although the most appropriate method of propagating uncertainties and sensitivities through the component models is currently unknown. A summary of the proposed compliance metrics for the integrated model are given in Table 9.

Table 9: Proposed compliance standards and metrics to satisfy the RA 5812 technical MECCs piloted SHOL assessment component of framework

MECC	Proposed Compliance Standards/Metrics
1.	• Extension of AS/SS model fidelity assessments as inputs to integrated system • NASA-STD-7009B M&S data pedigree factor
2.	• DIPES rating • Simulation fidelity rating
3.	Verification: • NASA-STD-7009B M&S verification factor Validation: • Embarked SHOL trial data and DIPES ratings
4.	• NASA-STD-7009B M&S uncertainty characterization factor
5.	• NASA-STD-7009B M&S results robustness factor

5.2 Integrated Model Development

The AS and SS models were integrated using the SAIF approach and toolset for piloted simulation mentioned in Section 3.2 [30]. For offline analysis, the SSM was integrated directly into the AS MATLAB/Simulink interface. The conceptual approach for both systems is diagrammed in Figure 16. The airwakes are interpolated from unstructured CFD data onto a structured grid and are then deployed as data lookup tables of airwake velocity components. At AS model runtime, the data are spatially and temporally interpolated to determine the airwake velocity perturbations at ACPs distributed over the aircraft flight dynamics model.

As required by RA 5812 MECC 3, verification checks were completed to ensure that integration of the airwakes with the AS was completed correctly. This is performed via cross-checking the airwake velocity components at the AS ACPs against the source CFD data. This includes checking that the airwake is correctly positioned relative to ship, moves appropriately with the ship, and blends appropriately to freestream wind conditions outside the airwake.

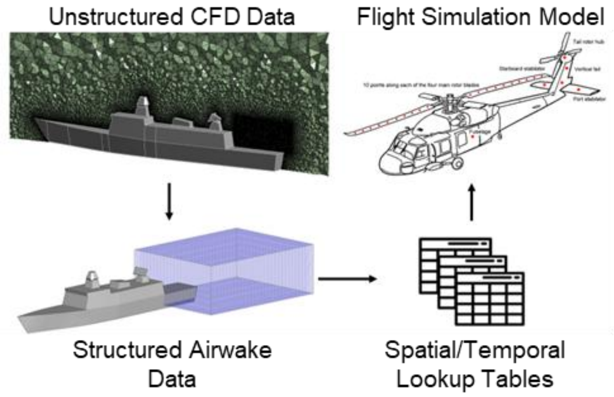

Figure 16: Process for integrating the ship airwakes with a flight dynamics model. Figure from Ref. [49].

5.3 Offline SHOL Prediction

As discussed in Section 1.1, SHOLs are typically defined by four factors that depend on relative wind azimuth over the ship (also discussed by Refs. [50] and [51]. The factors can be approximately attributed to four quadrants around the wind azimuth:

1. Pilot workload due to turbulence and deck motion (captured via DIPES), typically limits SHOL in the forward quadrant.
2. Pedal authority limits that arise in the left and right abeam quadrants due to the combined effects of steady-state trim and the transient control inputs required to maneuver and maintain stability.
3. Engine performance limits, primarily torque, typically limiting in aft quadrant.
4. Undercarriage limits for dynamic rollover typically encountered during high deck attitudes, and ultimate load limits most often encountered in winds from the aft quadrant.

To predict a SHOL without a pilot-in-the-loop, analysis must account for all these factors. The authors have constructed a process for predicting a SHOL boundary through offline analysis using a synthesis of tools previously developed by FS&T and new techniques to capture the various limiting factors. The process for offline SHOL prediction is diagrammed in Figure 17.

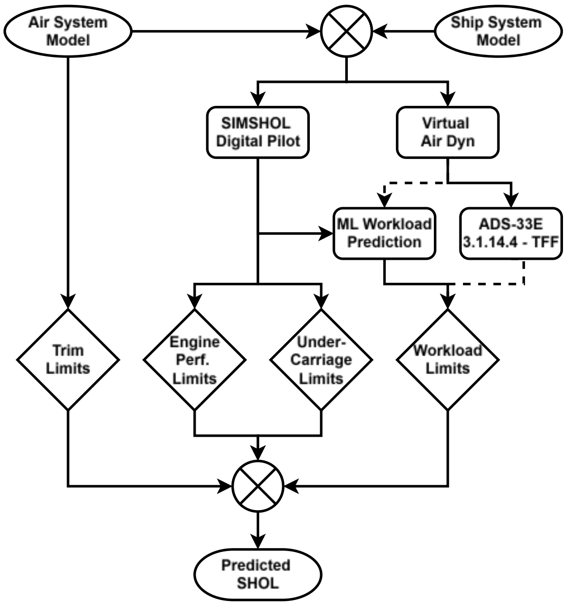

Figure 17: Offline SHOL prediction framework using existing FS&T-developed tools

The integration of the AS and SS models is followed by analysis with two primary tools: SIMSHOL, which integrates a pilot model with the AS and SS to perform recovery tasks [9], and the Virtual Air Dyn (VAD), which quantifies unsteady air loads on the AS [8]. Further tools are applied to their outputs: Machine Learning (ML) approaches to predicting the level of pilot workload from pilot control histories [52], and analysis via an ADS-33E criterion. The dashed line in the process (Figure 17) indicates a new approach that has yet to be validated, while solid lines are established processes. The data generated using these offline tools is combined with aircraft trim limits derived from the FSM, which define the steady-state pedal margins that will limit SHOL in some wind azimuths.

The SHOL prediction methodology was applied to the integrated AW159/Type 23 model described in Section 5.2. The resulting predicted SHOL is regarded as sensitive data so is not published here, but some of the key results produced from novel approaches are included in a non-dimensionalised form. The steady-state pedal trim margins were established via trim sweep of the FSM in varying wind conditions. Any condition that gave a pedal margin of less than 10% was deemed unacceptable as per Def. Stan 00-970 Part 7 requirement 2.3.3.1.

5.3.1 SIMSHOL Digital Pilot Model

SIMSHOL is a desktop-based predictive simulation tool for supporting SHOL analysis. It employs an integrated pilot-vehicle-environment model to execute SAI recovery tasks. The tool outputs equivalent data expected from an embarked or piloted simulation trial, including AS body states, engine performance and pilot control activity. The first iteration of SIMSHOL used a linear aircraft model with an e-CETI ship airwake, controlled by a multiloop structural pilot model, with an objective optimisation loop [53]. A complete description of the SIMSHOL architecture is outlined in Ref. [54]. For the present research, SIMSHOL has undergone significant development to integrate the full nonlinear FSM and SSM described in Sections 3.2 and 4.2 respectively. In the context of the four SHOL limiting factors, SIMSHOL allows investigation of transient control margins, engine performance and undercarriage loads on touchdown, but cannot capture pilot workload in isolation.

Previous research by FS&T has explored correlations between pilot control activity and workload using attack metrics but fell short of a cohesive model [55]. ML offers a novel approach to defining this link by uncovering patterns within the data. Ref. [52] describes a ML tool trained to predict the limit of pilot workload using control activity from past SAI recovery tasks. This tool is applied to the control responses generated using SIMSHOL in different WOD conditions, thereby predicting the operational boundary where pilot workload would cause a DIPES rating of 4 or 5 to be awarded, though it cannot predict discrete DIPES ratings.

The SIMSHOL tool was applied to the integrated AW159/Type 23 model to test transient control margins, torque limits and undercarriage loads. Full application of SIMSHOL to this aircraft is yet to be completed, dependent on more robust pilot model gain tuning and validation against piloted recovery control activity. Hence, further ML workload prediction is required on remaining SIMSHOL conditions.

While SIMSHOL has the potential to address all SHOL limiting factors, the pilot control activity predicted by SIMSHOL is unvalidated, so additional tools were sought to build confidence in the outputs.

5.3.2 Virtual Air Dyn

The FS&T's VAD tool was first reported on in Ref. [8]. The tool first trims the AS model in freestream conditions before positioning it at discrete locations within an airwake volume. At each point, the AS linear and rotational displacement states are frozen, which allows the resultant forces and moments induced by the SS airwake to be examined over time. Hence, the expected linear and rotational accelerations can be estimated, which can be used as an indicator of pilot workload when combined with other tools discussed below.

The outputs of the VAD can be assessed in multiple ways, including the 'Transient Following a Failure (TFF)' criteria detailed in ADS-33E-PRF [23]. This design standard states that any 'transient following a failure or combination of flight control system failures shall be recoverable to a safe steady flight condition without exceptional piloting skill'. Maximum values for transient attitude changes and linear accelerations are defined for each AS HQ level, given in Table 10.

Table 10: ADS-33E-PRF hover and low speed criteria for Transients Following a Failure [23].

HQ Level	Hover & Low Speed Requirements
1	Roll, pitch, yaw < 3°, n_x, n_y, n_z < 0.05g No recovery action for 3 s
2	Roll, pitch, yaw < 10°, n_x, n_y, n_z < 0.2g No recovery action for 3 s
3	Roll, pitch, yaw < 24°, n_x, n_y, n_z < 0.4g No recovery action for 3 s

The TFF criteria have been previously applied to an AS model encountering a wake vortex in Ref. [56], where it was reasoned that a wake encounter can cause similar excursions in state to an AS failure. This TFF analysis was applied in the present research using the VAD to determine the maximum attitudes and load-factors induced by the airwake, which were assessed against the hover and low speed TFF limits in each aircraft axis.

Table 11: Handling Quality Level Definitions [27].

Level	Description
1	Task achieved without excessive pilot workload.
2	Some degradation in task effectiveness or increase in pilot workload or both.
3	Aircraft can be controlled but with severe task degradation. The total workload of the pilot is approaching the limit of their capacity.
4	Inability to complete task required. Allowed only in special circumstances.

The HQ levels follow their standard definitions as per Table 11, which echo the levels defined by the Bedford workload rating scale. The level 2/3 boundary is also analogous to the DIPES 3/4 boundary that defines the acceptable SHOL boundary. This novel approach to workload limit prediction is thus far unvalidated, and a future simulator trial is planned to investigate whether a robust correlation exists.

The peak accelerations and angular displacement induced by the SS airwake on the AW159 FSM were assessed using this approach for a range of WOD conditions over a 30 second time period. All linear and angular axes were considered, but the most limiting case was in heave acceleration, which is typically the axis most affected by atmospheric turbulence.

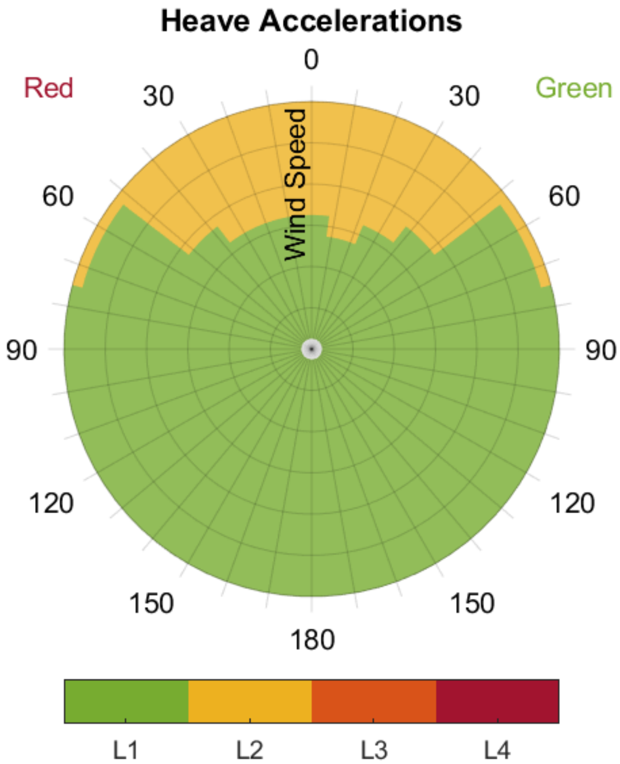

Figure 18: Handling qualities level according to the ADS-33E transients-following-a-failure criteria of the AW159 AS in varying wind-over-deck in the Type 23 SS airwake.

The resulting HQ levels per the TFF criteria are plotted across the WOD envelope in Figure 18, showing degradation in aircraft HQs to level 2 for increasing wind speed in the forward quadrant. However, no level 3 conditions were encountered in the tested condition, suggesting that the SHOL will not be limited by turbulence-induced pilot workload. Validation of this prediction is required via correlation with pilot opinion scales, which is planned for future phases of work.

The VAD outputs can also be analysed using statistical analysis to explore not only peak loads and displacements, but time-varying accelerations on the AS. Ref. [8] established that airwake disturbances that drove pilot compensation in the frequency range of 0.2-2Hz were the primary determiner of pilot workload, with higher frequency effects experienced as airframe vibration, and lower frequency effects a challenge for guidance rather stabilisation. This phenomenon can be analysed through the standard deviation of accelerations, computed via the integral of power spectral density of aircraft accelerations between the identified frequency limits. This approach has shown correlation of the statistical metrics with workload, but further work is required to define acceptable/unacceptable limits via this approach.

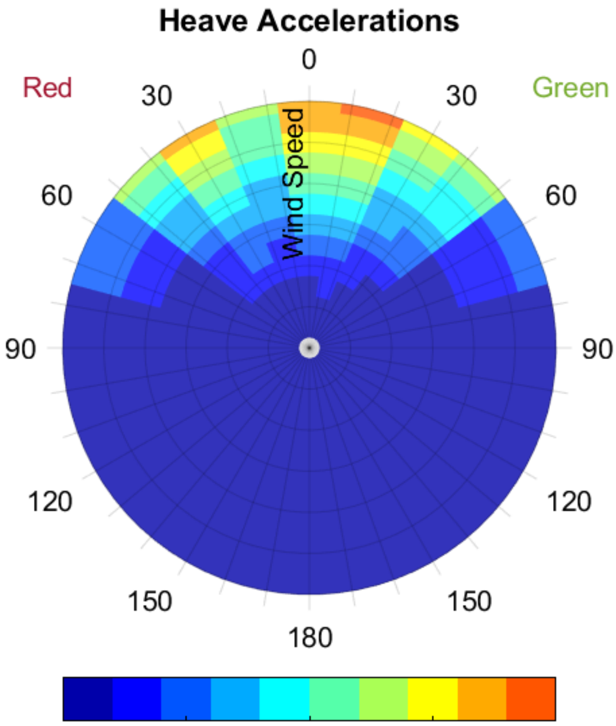

Figure 19: Standard deviation of heave acceleration in the 0.2-2 Hz frequency range of the AW159 AS in varying wind-over-deck conditions in the Type 23 SS airwake.

The same VAD results used for the TFF assessment were analysed using the statistical metrics, and the equivalent heave results are shown in Figure 19. Higher levels of standard deviation in acceleration are seen in the forward quadrant for increasing WOD speed as expected. This compares well with the TFF predictions and provides more detailed information but requires further work to correlate with workload boundaries. The ML approach used with SIMSHOL provides one avenue to defining this relationship, and outputs of piloted trials in the RCAT are currently being used to train a model that can identify pilot workload without the need for control activity data using that approach.

The limits predicted by each of the tools are then collated to estimate the SHOL boundary. This predicted SHOL can then be used to inform design of piloted simulation trials via identification of critical test points and can perform part of the evidence for SA-RLE or SA-R once validated against embarked trial data.

5.4 Integrated Model Fidelity Assessment

The inputs to the integrated model are the AS and SS models, so the input pedigree is based on the V&V performed for those components models, as described in Sections 3 and 4. Both models have shown some deficiencies against validation data, with the AS model generally assessed between a fidelity level 2 and 3 (warranting improvement/not fit for purpose), and the SSM exhibiting higher levels of airwake turbulence around the ships landing deck that were outside the fidelity bounds developed in Section 4.3. As such, the pedigree of inputs to the integrated model require improvements, which are planned for future phases of work. Per Section 5.2, verification of the integration was performed by cross-checking airwake velocities in CFD and through AS ACPs.To explore the validity of the integrated model and predicted SHOL, a piloted simulation trial was conducted in the HELIFLIGHT-R FS, again performing launch and recovery operations to the Type 23 frigate using the MTEs described in Section 4.3, but with an additional launch MTE included. The aims of the trial were to validate the integrated AS and SS models against embarked trial data through capture of DIPES and SFR ratings, and to determine the operational boundary for a candidate SHOL.

Several upgrades were made to the HELIFLIGHT-R FS in response to feedback from the first two simulator trials, including addition of a vibration cueing system, renovation of flying controls, a refactored instrument panel with more representative field of view, and improved audio and visual cueing. Improved visual cueing was achieved through development of new Unreal Engine 5-based image generation software, an example scene from which is shown in Figure 20.

Figure 20: HELIFLIGHT-R visual environment for piloted SHOL assessment

WOD condition, aircraft configuration and sea state of launch and recovery tasks were extracted from the embarked trial data set to define 15 validation points. The accompanying DIPES ratings and suffixes assigned to each condition served as the validation data. These points were repeated in the HELIFLIGHT-R by a team of four TPs, awarding DIPES and SFR ratings for each condition. SFRs were awarded against the TPs recollection of the RWS in the test condition, as one had also been a TP in the FoCFT for the Wildcat and Type 23. The awarded SFRs should be treated cautiously, as the pilots were intentionally not reminded of the RWS performance for that condition before rating. This choice was made to ensure that DIPES ratings were awarded 'blind' to avoid influencing TPs toward the RWS ratings. Hence, it was difficult for pilots to recall exact details of each WOD condition when awarding the SFR.

The variation in DIPES rating between RWS and simulator is graphed in Figure 21 on a typical polar SHOL plot. Green markers indicate that DIPES rating from the simulator trial matched the RWS, yellow markers indicate the rating was within 1 point, and red markers 2 points. DIPES ratings were mostly higher than the RWS with some significant variation in the suffixes awarded to denote causal factors in the rating. This is somewhat expected due the deficiencies identified in the AS and SS models, but a range of factors were captured well, particularly ship deck motion. From six conditions where deck motion was identified as a causal factor for the RWS DIPES rating, five were also identified as limited by deck motion in the FS.

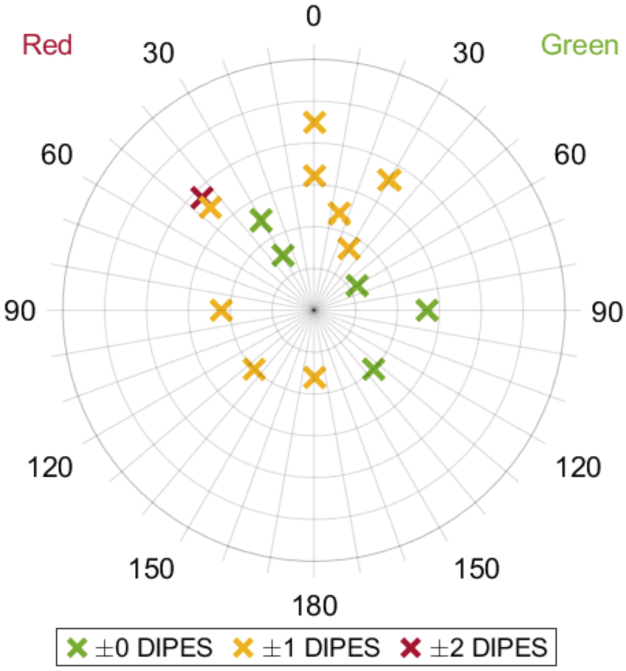

Figure 21: Difference in DIPES ratings between embarked and simulator trials for AW159 to Type 23 launch and recoveries.

SFRs awarded for the validation points varied between SFR 5 and 7, crossing the border into level 3 fidelity. The most consistently raised factors were collective sensitivity and deficient audio cueing, which reduced pilot confidence in collective strategy and torque management significantly. The level 3 ratings were generally awarded to conditions where the aircraft's heading hold functionality was saturated and the pilot had to make additional inputs, which they felt was not representative.

Following assessment of the fifteen validation points, further WOD conditions were assessed to evaluate where the SHOL boundary would sit. Interestingly, the boundary was found to be very similar to the in-service SHOL, even though DIPES ratings inside the envelope had been evaluated higher than the RWS. It is possible that the capability limit of the RWS is wider than the cleared SHOL but was limited by availability of conditions during embarked trials. This would go someway to explaining the difference in DIPES ratings, but similarity in SHOL boundaries. Further work is required to improve fidelity of the component AS and SS models to improve match of the validation points before the outputs of the integrated model can be applied for determining a candidate SHOL.

As previously discussed in Section 3.4, uncertainty and sensitivity analysis in the context of piloted simulation is a relatively unexplored area. This is especially true for the integrated model where uncertainties and sensitivities from both the component models are of concern. The level of effort required in this area must be discussed with regulators to inform further research. However, the integration process does create some unique sensitivities that should be analysed; the relative spacing of the airwake interpolation grid and spacing of aircraft ACPs can significantly affect response of the AS to SS airwake. This issue has been explored in Ref. [54], which concluded that ACP density should be equal to or greater than airwake grid spacing for best results. Increasing ACP density further did not affect AS response to the airwake. However, the most appropriate airwake grid resolution for aircraft of different sizes is yet to be explored. Grid sizing ultimately determines the size of flow structures that can be resolved, and while small flow structures may not affect large aircraft significantly, they may be more critical in modelling smaller, typically unmanned platforms. This sensitivity should be explored for future applications to platforms of different scales.

5.5 Integrated Model Summary

The component ship and air system models have been integrated and assessed via a new offline SHOL prediction process, as well as piloted simulations. Offline SHOL prediction integrates previously developed SIMSHOL and Virtual Air Dyn tools with new analysis techniques based on machine learning and HQ metrics. The pedigree of inputs to the integrated model is assessed as the propagated fidelity of the AS and SS models, so the deficiencies identified in Sections 3 and 4 reduce its credibility. Verification of the integration was performed via airwake spot checks and is considered well verified.

The integrated model was validated through a piloted simulation trial using DIPES ratings captured at sea as referent data. DIPES ratings in the FS exceeded embarked trial ratings by an average of 1 point. SFRs also indicated relatively low fidelity, attributed to the compounded deficiencies in the component models. Collective control response and audio cueing were identified as key fidelity issues and will be addressed in future development. Uncertainty and sensitivity of the defined validation metrics is challenging due to the number of contributing factors and has not been explored thus far. Further research and engagement with regulators is recommended to better scope future effort required.

6 CONCLUSIONS

The conclusions of the work presented thus far are as follows:

1. The regulatory environment in UK defence aviation is conducive to the use of M&S in clearance of aircraft operations to naval vessels. M&S offers significant potential for cost-savings and risk reduction in determination of Ship Helicopter Operating Limits (SHOL) for future aircraft/ship combinations.
2. A framework for generating evidence to support RTS/SA-R based on M&S has been proposed. The framework incorporates lessons from recent civil certification by simulation work, with independent fidelity assessment of the aircraft and ship models forming a critical foundation prior to integration for SHOL prediction.
3. Each component of the digital clearance framework has been discussed, and fidelity assurance standards have been drawn from existing literature wherever possible. The proposed standards have been selected to comply with the requirements of RA 5812, the MoD’s regulation governing use of M&S in airworthiness decision making.
4. A review of fidelity standards applicable to ship airwake models identified a lack of established criteria. In response, initial fidelity standards for airwake velocity and turbulence intensity have been defined following a piloted simulation experiment.
5. While this work is tailored to the UK defence aviation regulatory context, the proposed framework and compliance metrics are internationally recognized and should map to equivalent clearance processes in other countries.
6. A new process for predicting SHOL using offline tools has been proposed that does not rely on pilot-in-the-loop simulation. The process builds on existing tools developed by the authors, with new analysis techniques to bridge capability gaps. Further validation is required to establish its suitability for operational use.
7. A limited application of the proposed framework to an exemplar ship-helicopter pairing (the AW159 Wildcat and Type 23 frigate) has been presented, with reference to expected components of analysis defined in RA 5812. A range of deficiencies have been identified in the initial air and ship models which adversely affect validation of the integrated systems. Further work is

planned to develop and validate these models using the feedback mechanisms embedded in the digital clearance framework to build assurable evidence in support of SA-R.

Author contact:

Christopher Dadswell c.m.dadswell@liverpool.ac.uk

7 ACKNOWLEDGMENTS

The authors would like to gratefully acknowledge Leonardo Helicopters, Dstl and the MoD's Research, Development, Test & Evaluation department for funding this research. Furthermore, Leonardo Helicopters have provided both modelling and simulation capabilities and support throughout the project, enabling the application of these process-driven developments to a real-world system. Thanks is also given to the Rotary Wing Test and Evaluation Squadron (RWTES) for their support and input to conduct of simulator trials. Fraser Nash Consultancy have also supported this work with independent verification. The authors also acknowledge Ansys UK Ltd for the provision of Fluent licenses for academic research.

REFERENCES

[1] UK Ministry of Defence and MAA, "Regulatory Article (RA) 1395: Authorization to Permit Embarked Aviation in His Majesty's / MOD Ships," RA 1395 Issue 7, Dec. 2023.

[2] Royal Navy, "BRd 766 - Embarked Aviation Orders."

[3] S. J. Hodge, S. J. Zan, D. M. Roper, G. D. Padfield, and I. Owen, "Time-Accurate Ship Airwake and Unsteady Aerodynamic Loads Modeling for Maritime Helicopter Simulation," *J. Am. Helicopter Soc.*, vol. 54, Apr. 2009, doi: 10.4050/JAHS.54.022005.

[4] UK Ministry of Defence, "Defence Standard 00-133: Part 4 - Aviation Arrangements in Surface Ships: Acceptance of Aviation Arrangements," Apr. 2021, DEF STAN 00-133: Part 04.

[5] UK Ministry of Defence, "Defence Standard 00-970: Part 7 - Certification Specifications for Airworthiness: Rotorcraft," Ministry of Defence, DEF STAN 00-970 Part 7, Mar. 2021.

[6] J. S. Forrest, S. J. Hodge, I. Owen, and G. D. Padfield, "Towards fully simulated ship-helicopter operating limits: The importance of ship airwake fidelity," in *American Helicopter Society 64th Annual Forum*, Apr. 2008.

[7] I. Owen, M. D. White, P. Scott, R. Mateer, and M. Kelly, "Modelling and Simulation at The University of Liverpool in Support of UK Naval Aviation," in *American Society of Naval Engineers Launch and Recovery Symposium 2016*, Baltimore, USA, Nov. 2016.

[8] C. H. Kääriä, J. S. Forrest, and I. Owen, "The virtual AirDyn: a simulation technique for evaluating the aerodynamic impact of ship superstructures on helicopter operations," *Aeronaut. J.*, vol. 117, no. 1198, pp. 1233–1248, Dec. 2013, doi: 10.1017/S0001924000008836.

[9] W. A. Memon, I. Owen, and M. D. White, "Simshol: A predictive simulation approach to inform helicopter–ship clearance trials," *J. Aircr.*, vol. 57, no. 5, pp. 854–875, 2020, doi: 10.2514/1.C035677.

[10] J. S. Forrest, I. Owen, G. D. Padfield, and S. J. Hodge, "Ship-Helicopter Operating Limits Prediction Using Piloted Flight Simulation and Time-Accurate Airwakes," *J. Aircr.*, vol. 49, no. 4, pp. 1020–1031, Jul. 2012, doi: 10.2514/1.C031525.

[11] J. S. Forrest, "Predicting Ship-Helicopter Operating Limits using Time-Accurate CFD Ship Airwakes and Piloted Flight Simulation," The University of Liverpool, 2009.

[12] P. Scott, M. D. White, and I. Owen, "The Effect of Ship Size on Airwake Aerodynamics and Maritime Helicopter Operations," in *41st European Rotorcraft Forum*, Munich, Germany, Sep. 2015.

[13] R. Mateer, S. A. Scott, I. Owen, and M. D. White, "Superstructure Aerodynamics of the Type 26 Global Combat Ship," in *14th International Naval Engineering Conference (INEC)*, Glasgow, Oct. 2018. doi: 10.24868/issn.2515-818X.2018.038.

[14] N. A. Watson, I. Owen, and M. D. White, "Piloted Flight Simulation of Helicopter Recovery to the Queen Elizabeth Class Aircraft Carrier," *J. Aircr.*, vol. 57, no. 4, pp. 742–760, Jul. 2020, doi: 10.2514/1.C035733.

[15] UK Ministry of Defence and MAA, "Regulatory Article (RA) 5812: digital models and simulations supporting airworthiness-related decision-making," 2023. [Online]. Available: https://www.gov.uk/government/publications/regulatory-article-ra-5812-digital-models-and-simulations-supporting-airworthiness-related-decision-making

[16] National Aeronautics and Space

Administration (NASA), “NASA-STD-7009B,” 2024. [Online]. Available: https://standards.nasa.gov/standard/NASA/NASA-STD-7009

[17] The American Society of Mechnical Engineers (ASME), “ASME V&V 20-2009 (R2016), Standard for Verification and Validation in Computational Fluid Dynamics and Heat Transfer,” 2009.

[18] European Union Aviation Safety Agency (EASA), “CS-FSTD(H) Helicopter Flight Simulation Training Devices,” 2020.

[19] G. D. Padfield, S. Van, P. Hofmeister, L. Lu, M. White, and G. Quaranta, *Rotorcraft Certification by Simulation and Analysis An Introduction to the Principles*. Springer. doi: 10.1007/978-3-031-86398-1.

[20] DSTL, “RCloud Tasking Form – Part B: Statement of Requirement (SoR) for ROTORCRAFT CONCEPTS AND TACTICAL AVIATION RESEARCH.,” Requisition Number: RQ0000009013, SoR Version: 1.0, Dec. 2020.

[21] E. Timson, P. Perfect, M. White, G. Padfield, R. Erdos, and A. Gubbels, “Subjective fidelity assessment of rotorcraft training simulators,” in *American Helicopter society 68th Annual Forum*, Fort Worth, May 2012.

[22] UK Ministry of Defence and MAA, “Regulatory Article 1210 - Ownership and Management of Operating Risk (Risk to Life),” 2010. [Online]. Available: https://www.gov.uk/government/uploads/system/uploads/attachment_data/file/418893/RA1210_Issue_3.pdf

[23] U.S. Army, “Aeronautical Design Standard, Performance Specification, Handling Qualities Requirements for Military Rotorcraft,” United States Army Aviation and Missile Command, ADS-33E-PRF, Mar. 2000.

[24] P. Perfect, M. D. White, G. D. Padfield, and A. W. Gubbels, “Rotorcraft simulation fidelity: new methods for quantification and assessment,” *Aeronaut. J.*, vol. 117, no. 1189, pp. 235–282, 2013, doi: 10.1017/s0001924000007983.

[25] D. G. Mitchell, R. H. Hoh, H. Chengjian, and K. Strope, “Determination of maximum unnoticeable added dynamics,” *Collect. Tech. Pap. - 2006 Atmos. Flight Mech. Conf.*, vol. 2, no. August, pp. 938–953, 2006, doi: 10.2514/6.2006-6492.

[26] M. B. Tischler, “System Identification Methods for Aircraft Flight Control Development and Validation,” 1995.

[27] G. E. Cooper and R. P. Harper, “The Use of Pilot Ratings in the Evaluation of Aircraft Handling Qualities,” *Advis. Gr. Aerosp. Res. Dev. Neuilly-Sur-Seine*, vol. AGARD-567, pp. 1–56, 1969.

[28] L. Favaro, A. Rylko, and G. Quaranta, “Building Credible VTOL Flight Models for Handling Quality Certification by Simulation,” *Aerospace*, vol. 12, no. 6, 2025, doi: 10.3390/aerospace12060559.

[29] M. D. White, P. Perfect, G. D. Padfield, A. W. Gubbels, and A. C. Berryman, “Acceptance testing and commissioning of a flight simulator for rotorcraft simulation fidelity research,” *Proc. Inst. Mech. Eng. Part G J. Aerosp. Eng.*, vol. 227, no. 4, pp. 663–686, Apr. 2013, doi: 10.1177/0954410012439816.

[30] I. Cox, G. Turner, B. Finlay, and J. Duncan, “The ship/air interface framework (SAIF) project: Dynamic challenges, Maritime Operations of Rotorcraft,” in *RAeS Conference, 11-12 June.*, London, UK: Royal Aeronautical Society, 2008.

[31] UK Ministry of Defence, “Defence Imagery.” Accessed: Sep. 01, 2025. [Online]. Available: https://www.defenceimagery.mod.uk/Home/Search?Query=FLEET-20250203-XA00215-002.jpg&Type=Filename

[32] N. A. Watson, M. F. Kelly, I. Owen, S. J. Hodge, and M. D. White, “Computational and experimental modelling study of the unsteady airflow over the aircraft carrier HMS Queen Elizabeth,” *Ocean Eng.*, vol. 172, pp. 562–574, Jan. 2019, doi: 10.1016/j.oceaneng.2018.12.024.

[33] K. A. Mctaggart, “Verification and validation of ShipMo3D ship motion predictions in the time and frequency domains,” *Int. J. Nav. Archit. Ocean Eng.*, vol. 3, pp. 86–94, Mar. 2011, doi: 10.3744/JNAOE.2011.3.1.086.

[34] NATO, “Standardized Wave and Wind Environments and Shipboard Reporting of Sea Conditions,” STANAG 4194, 1983.

[35] J. S. Forrest, S. J. Hodge, I. Owen, and G. D. Padfield, “An investigation of ship airwake phenomena using time-accurate CFD and piloted helicopter flight simulation,” in *34th European Rotorcraft Forum 2008, ERF34*, 2008, pp. 1961–1971.

[36] N. Durrani and N. Qin, “Comparison of RANS, DES and DDES Results for ONERA M-6 Wing at Transonic Flow Speed Using an

In-House Parallel Code," in *49th AIAA Aerospace Sciences Meeting including the New Horizons Forum and Aerospace Exposition*, Orlando, Florida: American Institute of Aeronautics and Astronautics, Jan. 2011, pp. 1–13. doi: 10.2514/6.2011-190.

[37] P. R. Spalart, S. Deck, M. L. Shur, K. D. Squires, M. K. Strelets, and A. Travin, "A New Version of Detached-eddy Simulation, Resistant to Ambiguous Grid Densities," *Theor. Comput. Fluid Dyn.*, vol. 20, no. 3, pp. 181–195, Jul. 2006, doi: 10.1007/s00162-006-0015-0.

[38] J. S. Forrest and I. Owen, "An investigation of ship airwakes using Detached-Eddy Simulation," *Comput. Fluids*, vol. 39, pp. 656–673, Apr. 2010, doi: 10.1016/j.compfluid.2009.11.002.

[39] A. W. Gubbels, S. J. R. P. Carignan, and D. K. Ellis, "THE NRC BELL 412 ADVANCED SYSTEMS RESEARCH AIRCRAFT – FACILITY DESCRIPTION AND RESULTS OF INITIAL IN-FLIGHT EVALUATION," *Syst. Res.*, 2002.

[40] R. W. Du Val and C. He, "Validation of the FLIGHTLAB virtual engineering toolset," *Aeronaut. J.*, vol. 122, no. 1250, pp. 519–555, Apr. 2018, doi: 10.1017/aer.2018.12.

[41] B. Manimala, D. Walker, and G. Padfield, "Rotorcraft simulation modelling and validation for control design and load prediction," *31st Eur. Rotorcr. Forum*, vol. 2005, no. September, pp. 13–15, 2005.

[42] D. Agarwal, G. D. Padfield, M. D. White, N. Cameron, and L. Lu, "Rotorcraft simulation fidelity for low speed manoeuvring using 'additive' system identification," in *European Rotorcraft Forum 2019*,

[43] A. H. Roscoe and G. A. Ellis, "A Subjective Rating Scale for Assessing Pilot Workload in Flight: A Decade of Practical Use," RAE Technical Report 90019, 1990.

[44] ANSYS Inc., "ANSYS Release 2025 R2, Ansys Fluid Dynamics Verification Manual," 2025.

[45] Nortek AS, "The Comprehensive Manual Velocimeters," 2018, [Online]. Available: https://www.nortekgroup.com/assets/software/N3015-030-Comprehensive-Manual-Velocimeters_1118.pdf

[46] N. A. Watson, "The Validation and Application of CFD-generated Aircraft Carrier Airwakes for Flight Simulation," 2021.

[47] I. M. Stephens, "The Effect of Ship Exhaust Gas on Maritime Helicopter Operations," Liverpool, Oct. 2024.

[48] N. Fernandez, "CFD Analysis Approach for NATO-GD Airwakes," University of Liverpool, Jun. 2024.

[49] I. Owen, R. Lee, A. Wall, and N. Fernandez, "The NATO generic destroyer – a shared geometry for collaborative research into modelling and simulation of shipboard helicopter launch and recovery," *Ocean Eng.*, vol. 228, p. 108428, May 2021, doi: 10.1016/j.oceaneng.2020.108428.

[50] NATO RTO-AG-300, "Helicopter/Ship Qualification Testing," Neuilly-sur-Seine, France, RTO AGARDograph 300, Flight Test Techniques Series – Volume 22 Helicopter/Ship Qualification Testing, 2003.

[51] Task Group AVT-315, "Comparative Assessment of Modelling and Simulation Methods of Shipboard Launch and Recovery of Helicopters," STO-TR-AVT-315, Oct. 2024. doi: 10.14339/STO-TR-AVT-315.

[52] D. Newton-Young, M. White, and P. Green, "Use of Machine Learning Techniques to Support Future Ship-Helicopter Operations Research; an Initial Investigation," in *Proceedings of the Vertical Flight Society 80th Annual Forum*, The Vertical Flight Society, May 2024, pp. 1–10. doi: 10.4050/F-0080-2024-1378.

[53] R. A. Hess, "Structural Model of the Adaptive Human Pilot," *J. Guid. Control*, vol. 3, no. 5, pp. 416–423, Sep. 1980, doi: 10.2514/3.56015.

[54] W. A. Memon, "The Development of High-Fidelity Modelling & Simulation for the Helicopter Ship Dynamic Interface," 2019.

[55] W. A. Memon, M. D. White, G. D. Padfield, N. Cameron, and L. Lu, "Helicopter Handling Qualities: A study in pilot control compensation," *Aeronaut. J.*, vol. 126, no. 1295, pp. 152–186, Jan. 2022, doi: 10.1017/aer.2021.87.

[56] B. Lawrence and G. D. Padfield, "Wake vortex encounter severity for rotorcraft in final approach," *Aerosp. Sci. Technol.*, vol. 12, no. 5, pp. 385–397, Jul. 2008, doi: 10.1016/j.ast.2007.09.006.